Water Research 160 (2019) 313–329

Contents lists available at ScienceDirect

Water Research

journal homepage: www.elsevier.com/locate/watres

Review

Disinfection byproduct formation during drinking water treatment and distribution: A review of unintended effects of engineering agents and materials

Shunke Ding [a, b, c], Yang Deng [d], Tom Bond [e], Chao Fang [a, b, c], Zhongqi Cao [a, b, c], Wenhai Chu [a, b, c, *]

[a] State Key Laboratory of Pollution Control and Resources Reuse, College of Environmental Science and Engineering, Tongji University, Shanghai, 200092, China
[b] Key Laboratory of Yangtze River Water Environment, Ministry of Education, Tongji University, Shanghai, 200092, China
[c] Shanghai Institute of Pollution Control and Ecological Security, Shanghai, 200092, China
[d] Department of Earth and Environmental Studies, Montclair State University, Montclair, NJ, 07043, USA
[e] Department of Civil and Environmental Engineering, University of Surrey, Guildford, GU2 7XH, UK

ARTICLE INFO

Article history:
Received 27 February 2019
Received in revised form
6 May 2019
Accepted 7 May 2019
Available online 8 May 2019

Keywords:
Disinfection byproducts
Drinking water treatment
Drinking water distribution
Agents and materials
Unintended effect

ABSTRACT

Unintended effects of engineering agents and materials on the formation of undesirable disinfection byproducts (DBPs) during drinking water treatment and distribution were comprehensively reviewed. Specially, coagulants, biologically active filtration biofilms, activated carbons, nanomaterials, ion-exchange resins, membrane materials in drinking water treatment and piping materials, deposits and biofilms within drinking water distribution systems were discussed, which may serve as DBP precursors, transform DBPs into more toxic species, and/or catalyze the formation of DBPs. Speciation and quantity of DBPs generated rely heavily on the material characteristics, solution chemistry conditions, and operating factors. For example, quaternary ammonium polymer coagulants can increase concentrations of *N*-nitrosodimethylamine (NDMA) to above the California notification level (10 ng/L). Meanwhile, the application of strong base ion-exchange resins has been associated with the formation of *N*-nitrosamines and trichloronitromethane up to concentrations of 400 ng/L and 9.0 μg/L, respectively. Organic compounds leaching from membranes and plastic and rubber pipes can generate high NDMA (180–450 ng/L) and chloral hydrate (~12.4 μg/L) upon downstream disinfection. Activated carbon and membranes preferentially remove organic precursors over bromide, resulting in a higher proportion of brominated DBPs. Copper corrosion products (CCPs) accelerate the decay of disinfectants and increase the formation of halogenated DBPs. Chlorination of high bromide waters containing CCPs can form bromate at concentrations exceeding regulatory limits. Owing to the aforementioned concern for the drinking water quality, the application of these materials and reagents during drinking water treatment and distribution should be based on the removal of pollutants with consideration for balancing DBP formation during disinfection scenarios. Overall, this review highlights situations in which the use of engineering agents and materials in drinking water treatment and distribution needs balance against deleterious impacts on DBP formation.

© 2019 Elsevier Ltd. All rights reserved.

Contents

1. Introduction 314
2. Unintended effects of engineering agents and materials in drinking water treatment on DBP formation 315
   2.1. Coagulants 315

* Corresponding author. Room 308, Mingjing Building, 1239 Siping Road, Shanghai, 200092, China.
E-mail address: feedwater@126.com (W. Chu).

https://doi.org/10.1016/j.watres.2019.05.024
0043-1354/© 2019 Elsevier Ltd. All rights reserved.

Abbreviations of DBPs:

CF	Chloroform
BDCM	Bromodichloromethane
DBCAM	Dibromochloromethane
BF	Bromoform
DCIM	Dichloroiodomethane
BCIM	Bromochloroiodomethane
DBIM	Dibromoiodomethane
CDIM	Chlorodiiodomethane
BDIM	Bromodiiodomethane
IF	Iodoform
MCAA	Monochloroacetic acid
MBAA	Monobromoacetic acid
DCAA	Dichloroacetic acid
BCAA	Bromochloroacetic acid
DBAA	Dibromoacetic acid
TCAA	Trichloroacetic acid
BDCAA	Bromodichloroacetic acid
DBCAA	Dibromochloroacetic acid
TBAA	Tribromoacetic acid
CH	Chloral hydrate
1,1,1-TCP	1,1,1-trichloropropanone
1,1,1-DCP	1,1-dichloropropanone
MCNM	Monochloronitromethane
DCNM	Dichloronitromethane
DCAN	Dichloroacetonitrile
TCAN	Trichloroacetonitrile
MCAM	Chloroacetamide
DCAM	Dichloroacetamide
TCAM	Trichloroacetamide
BDCAM	Bromodichloroacetamide
DBCAM	Dibromochloroacetamide
TBAM	Tribromoacetamide
DIAM	Diiodoacetamide
NDMA	N-nitrosodimethylamine
NDPA	N-nitrosodipropylamine

2.1.1. PAM ... 315
2.1.2. PDADMAC and ECH/DMA ... 317
2.2. Biological filtration ... 318
2.3. AC ... 318
2.4. Nanomaterials ... 320
2.5. Ion-exchange resins ... 320
2.6. Membranes ... 321
3. Unintended effects of engineering agents and materials in drinking water distribution on DBP formation ... 321
3.1. Distribution system pipes ... 323
3.2. Distribution system deposits ... 324
3.3. Distribution system biofilms ... 325
4. Conclusions and implications for drinking water treatment and distribution ... 325
Acknowledgements ... 326
References ... 326

1. Introduction

Reliable access to safe and affordable water, as one of the most essential humanitarian goals, has remained a global challenge in the 21st century. As a consequence of unavailability of clean water, at a minimum, 1.8 million people, of whom 90% are under the age of 5, die due to water-related or waterborne diseases (e.g. diarrhea) every year (WHO, 2004). In order to combat pathogens in drinking water, efforts need to be made in two aspects. Firstly, effective disinfection is required for inactivation of pathogenic microorganisms during water treatment. Presently, chlorination is the most common disinfection option. Secondly, a sufficient disinfectant (e.g. chlorine) residual needs to be maintained within a water distribution system for prevention of the regrowth of unwanted microbes in finished water (Richardson et al., 2007; Richardson and Postigo, 2012; Sharma et al., 2017). However, many disinfectants, such as free chlorine, ozone, chlorine dioxide and chloramines, can potentially react with different water matrix constituents (e.g. natural organic matter (NOM), anthropogenic contaminants, bromide (Br^-), and iodide (I^-)) to generate undesirable disinfection byproducts (DBPs), which are cytotoxic, genotoxic and/or carcinogenic (Krasner et al., 2006; Richardson et al., 2007, 2008; Plewa et al., 2008; Yang and Zhang, 2014; Chu et al., 2016b; Ding et al., 2018c).

Since trihalomethanes (THMs) were first identified during chlorination of drinking water in 1974, significant efforts have been made to investigate occurrence, toxicity, formation mechanisms and mitigation technologies of various DBPs in water (Rook, 1974; Deborde and von Gunten, 2008; Bond et al., 2011; Shah and Mitch, 2012; Krasner et al., 2013). THMs, haloacetic acids (HAAs), and haloacetaldehydes (HALs) are three principal DBP classes typically ranging from several to a few hundreds of μg/L in finished water. In contrast, other DBPs such as haloacetonitriles (HANs), haloacetamides (HAMs) and halonitromethanes (HNMs) are formed at a much lower range from several ng/L to a few μg/L (Richardson et al., 2007; Bond et al., 2011; Wang et al., 2015). Besides the aforementioned halogenated DBPs, *N*-nitrosamines (NAs) represent a type of non-halogenated DBPs. The most well-known NA is *N*-nitrosodimethylamine (NDMA) with a typical concentration within several to a few tens of ng/L in finished water (Krasner et al., 2013; Bei et al., 2016). The US Environmental Protection Agency (USEPA) Integrated Risk Information System database indicates that the occurrence of 6 NAs in drinking water at several ng/L is associated with a 10^{-6} lifetime excess cancer risk. The notification level, which was set by California's Department of Public Health, for NDMA is 10 ng/L, several order lower than the regulated levels for THMs (80 μg/L) and HAAs (60 μg/L) (USEPA, 2006; CDPH, 2009). In general, the concentration levels of carbonaceous DBPs (C-DBPs),

are higher than that of nitrogenous DBPs (N-DBPs). However, systematic quantitative toxicological analyses of ~80 DBPs by Plewa and colleagues indicated that the N-DBPs are more toxic than C-DBPs (Muellner et al., 2007; Jeong et al., 2015). Moreover, some halogenated aromatic DBPs with higher toxicity than halogenated haloaliphatic DBPs were identified and quantified in various drinking water samples, ranged from several ng/L to a few μg/L (Pan and Zhang, 2013; Pan et al., 2014; Wang et al., 2018). Therefore, the toxic effect of N-DBPs and halogenated aromatic DBPs cannot be ignored because toxicity relies upon their concentration and toxic potency. Furthermore, the cytotoxicity and genotoxicity of DBPs are also highly influenced by the species of halogen substituted in the DBP compounds with the following order: iodo- > bromo- ≫ chloro- (Plewa et al., 2008).

Previous studies on the precursors of DBPs in drinking water treatment have primarily focused on NOM and anthropogenic contaminants originally present in raw water (Korshin et al., 2007; Deborde and von Gunten, 2008; Bond et al., 2012; Shah and Mitch, 2012). Among these precursors, phenolic structures identified in humic acids (HAs) and fulvic acids have been recognized as the principal precursors of THMs and HAAs, while amino acids, oligopeptides, and nitrogen-containing contaminants serve as the major N-DBP precursors (Gallard and von Gunten, 2002; Lee and Westerhoff, 2006; Chu et al., 2010; Yang et al., 2010; Bond et al., 2012; Chu et al., 2015b; Ding et al., 2018b). However, in many cases, concentrations of the known precursors in raw water cannot be sufficiently transformed to experimentally measured DBPs in finished waters (Bond et al., 2012). Therefore, the recent interest has been directed to other DBP precursors. These alternative chemical constituents in water may be those originally existing in raw water or may be treatment agents externally added and chemicals released from treatment and piping materials (Bolto and Gregory, 2007; Krasner et al., 2013; Sharma et al., 2017). Recent studies have highlighted the role of different chemical agents and treatment/piping materials on the DBP formation (Mitch and Sedlak, 2004; Padhye et al., 2011; Verdugo et al., 2014; Du et al., 2016). Besides the additional DBP precursors, another emerging concern is that certain treatment steps have the potential to transform existing DBPs into more toxic compounds. For example, activated carbon (AC), ion-exchange resins or membrane treatments can increase the ratios of brominated DBPs (Br-DBPs) to chlorinated DBPs (Cl-DBPs), resulting in greater mammalian cell cytotoxicity and genotoxicity, although the overall DBP concentrations decrease (Chellam and Krasner, 2001; Kemper et al., 2009; Krasner et al., 2016b; Zhang et al., 2017).

This article provides a critical review on the unintended effects of drinking water treatment reagents and treatment/piping materials on the DBP formations. The unwanted effects include: 1) alternative DBP precursors; 2) transformation of DBPs into more toxic species; and 3) catalysis of DBP formation.

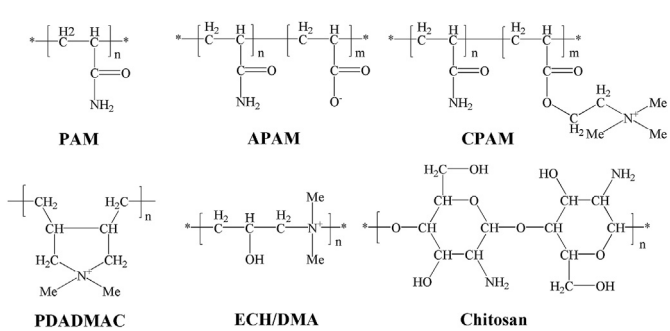

Fig. 1. Structures of PAM, APAM, CPAM, PDADMAC, ECH/DMA and Chitosan.

2. Unintended effects of engineering agents and materials in drinking water treatment on DBP formation

2.1. Coagulants

Coagulation is a process where the addition of an inorganic or organic coagulant for destabilizing particular matter, for promoting their aggregation or for forming precipitates that can sweep particulates in water (Matilainen et al., 2010). Organic polyelectrolytes (Fig. 1) have been widely applied as coagulants or coagulant aids for promoting the coagulation performance in water treatment, such as polyacrylamide (PAM), anion PAM (APAM), cation PAM (CPAM), poly(diallyldimethylammonium chloride) (PDADMAC), and epichlorohydrin/dimethylamine (ECH/DMA) (Bolto and Gregory, 2007). Benefits of these organic treatment agents include an excellent coagulation efficiency achieved at a low coagulant dose, the production of less sludge, no reduction in alkalinity, and a low cost (ca. 70–75% of the costs associated with inorganic coagulants) (Bolto and Gregory, 2007). However, the amide, quaternary amine and primary amine groups on these compounds and their monomers can react with several disinfectants to produce toxic N-DBPs (Bolto and Gregory, 2007; Krasner et al., 2013).

2.1.1. PAM

Formation of THMs from the reactions of chlorine with PAM, APAM, CPAM or their monomers, e.g. acrylamide (AM), has been reviewed (Bolto, 2005). These reactions can produce THMs at several μg/mg in ultrapure water (Table 1) (Klaus and Lawrence, 1977; Feige et al., 1980; Soponkanaporn and Gehr, 1988). The presence of AM, as an impurity of PAM, can greatly enhance the formation of THMs, because 1 mg/L of AM can produce 800 μg/L CF in ultrapure water (Mallevialle et al., 1984). Thus, it is of importance to increase the purity of PAM products during manufacture or adopt high-purity PAM coagulants for water treatment. Under the treatment conditions related to water treatment, the dose of AM based coagulant is typically less than 1 mg/L and the residual polymer coagulant after filtration is quite low (Bolto and Gregory, 2007). Consequently, the formation of THM due to the presence of residual PAM compounds is minor. Therefore, the use of AM based coagulant does not greatly contribute to the production of THMs in comparison with NOM in water during chlor(am)ination (Richardson et al., 2007; Ding et al., 2018a).

Recent studies validate that PAM and AM can also serve as the precursors of N-DBPs which are much more toxic than THMs (Plewa et al., 2008). Li et al. (2017) compared the formation of NAs during coagulation with different coagulants, including $Al_2(SO_4)_3$ alone and in combination of $Al_2(SO_4)_3$ and PAM, followed by chloramination. Results showed that the addition of 2 mg/L PAM as the coagulant aid only increased the formation of total NAs (TONO) from 75 ng/L to 80 ng/L and NDMA from 26 ng/L to 29 ng/L, separately. The subsequent DBP formation potential (FP) experiments revealed that 1 mg/L of PAM could produce 8 ng/L NDMA and 20 ng/L TONO. The enhanced removal of NA precursors and the sedimentation of partial PAM inhibits the rate of TONO and NDMA increase. Because the typical AM dose and residual AM concentration are typically low in realistic water coagulation, PAM cannot significantly increase the formation of TONO and NDMA in practice. Moreover, PAM and APAM exhibit much less FP of NDMA than that of PDADMAC due to less abundant dimethylamine (DMA) groups (Krasner et al., 2013). However, the NDMA yield of DMA-based CPAM is approximately greater than that of DMA by two orders of magnitude after 4 h chloramination (12.1 ± 4.3 μg NDMA/mg DMA based CPAM), indicating a high potential of the DMA-based CPAM in the enhanced formation of NDMA (Mitch and Sedlak, 2004). Therefore, the application of DMA based CPAM in drinking water

Table 1
DBP formation yields during chlor(am)ination of polymer coagulants.

Coagulants	DBP species	Reaction conditions	Yields (μg DBP/ mg Coagulant)	References
PAM	TCM	PAM = 3.55 mg/L, Cl_2 = 17.75 mg/L, pH = 6.0 (10 mM phosphate), time = 24 h, and 25 ± 0.5 °C.	1.36	Ding et al., (2018a)
		PAM = 3.55 mg/L, NH_2Cl = 17.75 mg/L, pH = 6.0 (10 mM phosphate), time = 24 h, and 25 ± 0.5 °C.	3.68	
		PAM = 10 mg/L, Cl_2 = 10 mg/L, time = 1 h, and UV irradiation.	0.18	Klaus and Lawrence, (1977)
		PAM = 1 mg/L, Cl_2 = 10 mg/L, time = 1 h, and UV irradiation.	0	
		PAM (1) = 1 mg/L, Cl_2 = 5 mg/L, time = 72 h, and room temperature.	7.7	Feige et al., (1980)
		PAM (1) = 1 mg/L, Cl_2 = 10 mg/L, time = 72 h, and room temperature.	9.2	
		PAM (2) = 1 mg/L, Cl_2 = 5 mg/L, time = 72 h, and room temperature.	1.2	
		PAM (2) = 1 mg/L, Cl_2 = 50 mg/L, time = 72 h, and room temperature.	3.3	
	DCAN	PAM = 3.55 mg/L, Cl_2 = 17.75 mg/L, pH = 6.0 (10 mM phosphate), time = 24 h, and 25 ± 0.5 °C.	0.14	Ding et al., (2018b)
		PAM = 3.55 mg/L, NH_2Cl = 17.75 mg/L, pH = 6.0 (10 mM phosphate), time = 24 h, and 25 ± 0.5 °C.	0.13	
	DCAM	PAM = 3.55 mg/L, Cl_2 = 17.75 mg/L, pH = 6.0 (10 mM phosphate), time = 24 h, and 25 ± 0.5 °C.	5.23	
		PAM = 3.55 mg/L, NH_2Cl = 17.75 mg/L, pH = 6.0 (10 mM phosphate), time = 24 h, and 25 ± 0.5 °C.	6.04	
	NDMA	PAM = 3 mg/L, NH_2Cl = 4.5 mg/L, pH = 8.0 (4 mM borate), time = 72 h, and 25 °C.	0.008	Li et al., (2017)
AM	TCM	AM = 1 mg/L, Cl_2 = 5 mg/L, and time = 24 h.	800	Mallevialle et al., (1984)
		AM = 10.95 mg/L, Cl_2 = 106.5 mg/L, pH = 7.0 (10 mM phosphate), time = 24 h, and 25 ± 1 °C.	1.46	Wang et al., (2018)
	DCAN	AM = 3.65 mg/L, Cl_2 = 17.75 mg/L, pH = 6.0 (10 mM phosphate), time = 24 h, and 25 ± 0.5 °C.	0.22	Ding et al., (2018c)
		AM = 3.65 mg/L, NH_2Cl = 17.75 mg/L, pH = 6.0 (10 mM phosphate), time = 24 h, and 25 ± 0.5 °C.	0.17	
	DCAM	AM = 3.65 mg/L, Cl_2 = 17.75 mg/L, pH = 6.0 (10 mM phosphate), time = 24 h, and 25 ± 0.5 °C.	3.66	
		AM = 3.65 mg/L, NH_2Cl = 17.75 mg/L, pH = 6.0 (10 mM phosphate), time = 24 h, and 25 ± 0.5 °C.	1.78	
		AM = 10.95 mg/L, Cl_2 = 106.5 mg/L, pH = 7.0 (10 mM phosphate), time = 24 h, and 25 ± 1 °C.	2.47	Wang et al., (2018)
APAM	TCM	APAM = 4 mg/L, Cl_2 = 50 mg/L, time = 72 h, and 20 °C.	14.5	Feige et al., (1980)
	BDCM	APAM = 4 mg/L, Cl_2 = 5 mg/L, time = 72 h, and 20 °C.	6	
	BDCM	APAM = 1–5 mg/L, Cl_2 = 2–10 mg/L, time = 1–24 h, and 20 °C.	1.6–8	Mallevialle et al., (1984)
		APAM = 40 mg/L, Cl_2 = 20 mg/L, time = 72 h, and 20 °C.	1.75	
		APAM = 40 mg/L, Cl_2 = 50 mg/L, time = 72 h, and 20 °C.	2.35	
		APAM = 40 mg/L, Cl_2 = 20 mg/L, time = 72 h, and 20 °C.	0.01	Feige et al., (1980)
		APAM = 40 mg/L, Cl_2 = 50 mg/L, time = 72 h, and 20 °C.	0.02	
CPAM	TCM	CPAM = 10 mg/L, Cl_2 = 20 mg/L, pH = 7, time = 20 days, and room temperature.	2.8	Soponkanaporn and Gehr, (1988)
		CPAM = 10 mg/L, Cl_2 = 20 mg/L, pH = 9, time = 20 days, and room temperature.	14.5	
	NDMA	CPAM = 11.6 mg/L, NH_2Cl = 7 mg/L, pH = 6.9 ± 0.4 (10 mM phosphate), time = 4 h, and room temperature.	12.06	Mitch and Sedlak, (2004)
		CPAM = 10 mg/L, Ozone = 6.7 mg/L, pH = 7.6 (5 mM phosphate and 1 mM carbonate), time = 0.5 h, and 23 ± 1 °C.	0.028	Padhye et al., (2011)
PDADMAC	TCM	PDADMAC = 10 mg/L, Cl_2 = 2 mg/L, pH = 7, and time = 24 h.	0.15	Klaus and Lawrence, (1977)
		PDADMAC = 10 mg/L, Cl_2 = 2 mg/L, pH = 7, time = 2 h, and UV irradiation.	0.31	
		PDADMAC = 100 mg/L, Cl_2 = 10 mg/L, pH = 7, and time = 4 h.	0.024	
		PDADMAC = 100 mg/L, Cl_2 = 10 mg/L, pH = 7, time = 1 h, and UV irradiation.	0.29	
		PDADMAC = 2 mg/L, Cl_2 = 25 mg/L, pH = 7, and time = 4 h.	0.5	Fielding et al., (1999)
	NDMA	PDADMAC = 6000 mg/L and Cl_2 = 5000 mg/L.	0.0002–0.0012	Child et al., (1996)
		PDADMAC = 0.5 mg/L, Cl_2 = 1.5 mg/L, and time = 20 h.	< 0.02	
		PDADMAC = 5 mg/L, Ozone = 1–10 mg/L, pH = 7.6 (5 mM phosphate and 1 mM carbonate), and 23 ± 1 °C.	0.016–0.04	Padhye et al., (2011)
		PDADMAC (50 000 < MW < 200 000 g/mol) = 10 mg/L, NH_2Cl = 10 mg/L, pH = 7.5, time = 24 h, and 23 °C.	0.045	Park et al., (2009)
		PDADMAC (300 000 < MW < 1 000 000 g/mol) = 10 mg/L, NH_2Cl = 10 mg/L, pH = 7.5, time = 24 h, and 23 °C.	0.038	
		PDADMAC = 10 mg/L, NH_2Cl = 141 mg/L, pH = 6.9 (10 mM phosphate), time = 10 d, and room temperature.	0.8–1.1	Zeng et al., (2014)
		PDADMAC = 1.5 mg/L, pH = 8 (2 mM borate), time = 24 h, and 25 °C.	0.09–0.18	Hanigan et al., (2015)
		PDADMAC = 1.5 mg/L, chlorination with 2.5 mg/L-Cl_2 residual followed by the addition of ammonia with a Cl_2/N weight ratio of 4.75:1 mg/mg, pH = 8, time = 72 h, and 25 °C.	0.031–0.13	Cornwell et al., (2017)
ECH/DMA	TCM	ECH/DMA = 100 mg/L, Cl_2 = 10 mg/L, pH = 7, time = 1 h, and UV irradiation.	0.14	Klaus and Lawrence, (1977)
		ECH/DMA = 10 mg/L, Cl_2 = 5 mg/L, and time = 72 h.	0.36	Feige et al., (1980)
		ECH/DMA = 10 mg/L, Cl_2 = 10 mg/L, pH = 7, and time = 72 h.	0.63	
		ECH/DMA = 10 mg/L, Cl_2 = 50 mg/L, pH = 7,and time = 72 h.	3.4	
		ECH/DMA = 5 mg/L, Cl_2 = 25 mg/L, pH = 7, and time = 4 h.	0.74	Fielding et al., (1999)
	NDMA	ECH/DMA = 10 mg/L, Ozone = 6.7 mg/L, pH = 7.6 (5 mM phosphate and 1 mM carbonate), time = 0.5 h, and 23 ± 1 °C.	0.02	Padhye et al., (2011)
		ECH/DMA (MW < 50 000 g/mol) = 10 mg/L, NH_2Cl = 10 mg/L, pH = 7.5, time = 24 h, and 23 °C.	0.89	Park et al., (2009)
		ECH/DMA (20 000 < MW < 80 000 g/mol) = 10 mg/L, NH_2Cl = 10 mg/L, pH = 7.5, time = 24 h, and 23 °C.	0.17	
		ECH/DMA (300 000 < MW < 1 000 000 g/mol) = 10 mg/L, NH_2Cl = 10 mg/L, pH = 7.5, time = 24 h, and 23 °C.	0.16	
		ECH/DMA = 1.5 mg/L, pH = 8 (2 mM borate), time = 24 h, and 25 °C.	0.35	Hanigan et al., (2015)
Chitosan	NDMA	Chitosan = 3 mg/L, NH_2Cl = 4.5 mg/L, pH = 8.0 (4 mM borate), time = 72 h, and 25 °C.		Li et al., (2017)

treatment should be carefully evaluated before adoption.

Contribution of PAM to the formation of HAMs, HANs, and THMs was recently investigated (Ding et al., 2018a). Coagulation with PAM did not greatly promote the formation of THMs and HANs in the downstream post-chlorination, suggesting that the role of PAM residuals for the overall THM and HAN formation is insignificant. However, coagulation with combined $Al_2(SO_4)_3$ (10 mg/L as alum) and PAM (2 mg/L) increased total HAM concentrations by 40–96%, corresponding to 4.9–7.7 μg/L HAMs, in comparison with those produced from coagulation with alum alone (2.5–5.5 μg/L HAMs). Moreover, the DBP FP experiments revealed that chlorination following coagulation with 1 mg/L PAM produced 5.2 μg/L DCAM. Therefore, the potential of the PAM residual in the formation of HAMs is close to that of NOM. It should be noted that the DBP associated toxicity in water is a function of both its concentration and its toxic potency. Even though the concentration of HAMs is less than that of THMs nearly by one order of magnitude, the CHO cell cytotoxicity of HAMs is greater than that of THMs by several orders of magnitude (Wagner and Plewa, 2017). After considering the two factors, it is concluded that the health risk associated with HAMs formed from residual PAM is close to or even greater than that of THMs transformed from NOM in water.

2.1.2. PDADMAC and ECH/DMA

A review on the formation of THMs from the chlorination of PDADMAC and ECH/DMA indicates that the THM yield of PDADMAC or ECH/DMA is substantially lower than that of CPAM under identical water treatment conditions (Table 1) (Bolto, 2005). However, a concern has been raised since NDMA was identified in the water treated with PDADMAC and chlorine (Child et al., 1996; Kohut and Andrews, 2003; Bolto, 2005; Park et al., 2009; Krasner et al., 2013). As shown in Table 1, the NDMA yields from chlorination of PDADMAC range from 0.2 to 1.2 ng NDMA/mg polymer (Child et al., 1996). Later, studies showed that the NDMA yields from reactions of PDADMAC or ECH/DMA with chlorine or ozone were substantially below those produced from chloramines (Najm and Trussell, 2001; Wilczak et al., 2003). NDMA after chloramination of PDADMAC or ECH/DMA was reported to reach several μg NDMA/mg coagulant (Table 1). Hanigan et al. (2015) reported that coagulation with 1.5 mg/L PDADMAC in 7 water samples across the U.S. led to the formation of 47 ± 3 ng NDMA/mg active polymer during the downstream chloramination. Although the NDMA yields were approximately one-third of the NDMA FP (129 ng NDMA/mg PDADMAC) measured in ultrapure water (Hanigan et al., 2015), the NDMA concentrations far exceeded the California notification Level (10 ng/L) (CDPH, 2009). The USEPA Integrated Risk Information System database indicates that the occurrence of 6 NAs in drinking water at several ng/L is associated with a 10^{-6} lifetime excess cancer risk. Moreover, application of PDADMAC during coagulation frequently increased the NDMA FP during ensuing chloramination water, regardless of the disinfectant dose, suggesting that an optimal coagulant dose should be selected based on the trade-off between turbidity removal and NDMA formation (Hanigan et al., 2015). Furthermore, NDMA concentrations formed from the chloramination of coagulated waters with PDADMAC or ECH/DMA can be similar to those formed from the chloramination of wastewater effluent or reclaimed water, which are known to be important sources of NDMA precursors (Le Roux et al., 2011; Parker et al., 2014; Sgroi et al., 2015; Chuang and Mitch, 2017; Chuang et al., 2019).

Park et al. (2009) reported that ECH/DMA had a greater NDMA yield than PDADMAC and the formation of NDMA from the both polymers was strongly correlated to the polymer degradation and DMA release during chloramination. Two chloramine dosing modes, i.e. direct addition of preformed chloramines and simultaneous addition of chlorine and ammonia, favor the formation of NDMA, compared with addition of free chlorine before ammonia. And the concentration of NDMA decreases with the increase of pre-chlorination time (Wilczak et al., 2003). Therefore, pre-chlorination appears to be effective for the reduction of NDMA FP of PDADMAC or ECH/DMA. During *in situ* chloramination, dichloramine ($NHCl_2$) formation plays a critical role in the formation of NDMA from the aforementioned polymers (Park et al., 2015). Moreover, pre-oxidation with ClO_2 also reduces the formation of NDMA from PDADMAC and ECH/DMA, whereas pre-ozonation favors its production (Selbes et al., 2014; Park et al., 2015). The different findings are due to the fact that hydroxyl radicals (•OH) generated from ozonation can break down the quaternary ammonium ring on PDADMAC following by the release of DMA, which can later form NDMA during downstream chloramination (Padhye et al., 2011). Furthermore, the reaction of hydroxylamine, another ozonation product of DMA, with DMA can also directly generate NDMA during ozonation (Padhye et al., 2011). Therefore, the application of PDADMAC before disinfection with ozone and $NHCl_2$ should be avoided for the minimization of the NDMA formation. Additionally, the stock age of coagulants is a factor likely affecting the DBP formation in subsequent disinfection. Kohut and Andrews (2003) found that the stock age of PDADMAC did not significantly alter the NDMA production, whereas the NDMA concentration was appreciably increased when the stock age of ECH/DMA increased from 0 to 5 h.

In order to inhibit the formation of NAs, Zeng et al. (2016) attempted to modify PDADMAC and ECH/DMA. In the first modification pathway, methyl iodide (MeI) was used to convert polymer-bound tertiary amine groups to less chloramine-reactive quaternary ammonium groups on the polymer. The modification could reduce the NDMA formation approximately by 75%. In the other modification method, the chloramine-reactive DMA group was converted to longer alkyl substituents (i.e. dipropylamine (DPA) substituents), completely eliminating the NDMA formation in the following disinfection. The yields of *N*-nitrosodipropylamine (NDPA) from DPA based polymers were 5% of the NDMA yields from DMA based polymers. Zeng et al. (2016) reported that chloramination of water coagulated with the combination of untreated PDADMAC or ECH/DMA (2.0 mg/L) with alum or ferric salts increased the yields of NDMA by 6–17 times (38–101 ng/L) and TONO by 2–3 times (76–135 ng/L) in comparison with their respective yields when chloramination of water coagulated with alum or ferric salt alone. NDMA was the dominant NA species produced from these polymers. Coagulation with DPA-based analogues of PDADMAC or ECH/DMA produced less NDMA and TONO than coagulation with MeI-treated polymers. However, coagulation with the aforementioned modified polymers also produced more NDMA and TONO. Zeng et al. (2014) synthesized a novel quaternary phosphonium cationic polymer, i.e. poly (diallyldiethylphosphonium chloride) (PDADEPC), which could achieve comparable turbidity and NOM removals with commercial PDADMAC. Moreover, chloramination of PDADEPC primarily produced oxygenated products rather than nitrosated products even under strong nitrosation conditions. This could be achieved by converting the chloramine-reactive DMA group to longer alkyl substituents (i.e. DEP) substituents. One study found that powdered and granular activated carbon (PAC and GAC) could effectively remove ECH/DMA (up to 75%) compared to PDADMAC (Hanigan et al., 2015). Therefore, AC adsorption, when ECH/DMA is applied before polymer addition and/or after sedimentation, is a potential method to inhibit the NDMA formation.

In summary, the NDMA FP or HAM FP of the waters coagulated with the quaternary ammonium polymer coagulants or AM based coagulants is potentially high. Therefore, adoption of these

coagulants has a risk to produce NAs and HAMs at undesirable levels.

2.2. Biological filtration

Biological active filtration (BAF) is designed to remove not only particles but also dissolved organic matters by microbial, growing in the form of biofilm attached to a support media (Bablon et al., 1988; Hu et al., 2018). Recently, Liu et al. (2017) reviewed the impact of BAF on the control of DBP precursors and DBPs and demonstrated that biofiltration generally can enhance the removal of the precursors of DBPs. However, some studies also indicated that BAF process can also increase the formation of NAs and halogenated N-DBPs under certain conditions (Chu et al., 2011, 2015a). Chu et al. (2011) reported that, compared to conventional drinking water treatment, BAF pretreatment resulted in the increases of DCAN, DCAM and TCNM by 43.3%, 115.4% and 33.3% to 8.6 μg/L, 5.6 μg/L and 1.6 μg/L, respectively. Chu et al. (2015a) investigated the impact of pre-ozonation on the ability of the coupling pre-ozonation with biological activated carbon (O_3-BAC) to remove the N-DBP precursors. Results showed that, when the pre-ozonation was terminated after the first backwash cycle, DCAN, TCAN, DCAM and TCAM concentrations were 21.3%, 19.6%, 33.5% and 53.7% higher than that in the chlorinated effluent of the O_3-BAC. Moreover, other studies also observed an increase of NA precursors after biofiltration. Krasner and colleagues found that the removal of NDMA precursors by biofiltration ranged from −344% to 50% of 37 full-scale water treatment BAF effluents compared to BAF influents (Krasner et al., 2015, 2016a). The negative removal of NDMA precursors were observed in 22 samples, indicating the increase in NDMA FP after BAF treatment. The increases of N-DBPs may be ascribed to the biomass sloughing off from the biofilter and/or the release of soluble microbial products (Chu et al., 2011, 2015a; Liu et al., 2017). On the one hand, bacterial cells in the BAF biofilms, bacterial extracellular polymeric substances, intracellular organic matter in cyanobacteria, and soluble microbial products can all provide reactive DBP precursors (Chu et al., 2011, 2015a; Liu et al., 2017). In addition to generating organic nitrogen compounds, microbial mediated processes (nitrification) can also enhance the formation of NDMA in the presence of inorganic nitrogen species (Zeng and Mitch, 2016). Moreover, the desorption of cationic polymers and other positively-charged amine based precursors from BAF can release existing DBP precursors and in this way also contribute to DBP FP (Liao et al., 2015). Overall, during biological filtration, there are a number of processes which it may enhance DBP formation. However, the increase of N-DBP precursors after biofiltration appeared to be site-specific and need to be comprehensively investigated in future studies. It is necessary to investigate the dominant factors which determine increases or decreases in N-DBP precursors, in future research.

2.3. AC

Adsorption in drinking water treatment is a surface process in which atoms, ions, or molecules (i.e. adsorbates) are accumulated on the surface of a solid (i.e. adsorbent). AC is the most popular adsorbent applied for environmental purification purposes, particularly capturing traceable micro-pollutants in drinking water treatment. The AC serving as adsorbent can be categorized into cylindrical AC, granular AC (GAC), powder AC (PAC) and AC fiber in terms of their shape and appearance (Padhye et al., 2010; Bond et al., 2012; Krasner et al., 2016b). The excellent adsorption ability of AC is ascribed to its large specific surface area, well-developed pore structures, and abundant surface functional groups (Li, 2012).

AC adsorption has served as an effective barrier for the abatement of DBP precursors such as NOM. Chiu et al. (2012) reported the simultaneous and effective removals of dissolved organic carbon (DOC), ultraviolet absorbance at 254 nm (UV_{254}), total dissolved nitrogen (TDN), dissolved inorganic nitrogen (DIN), dissolved organic nitrogen (DON), and Br^- using rapid small-scale column tests (RSSCTs) loaded with GAC for water treatment. As shown in Fig. 2, the capability of GAC in the alleviation of different water quality indicators follows the order: UV_{254} absorbance > DOC > DON > TDN > Br^-. The better removal efficiency of UV_{254} absorbance than the removal of DOC suggests that GAC preferentially captures aromatic NOM molecules with typically higher UV_{254} absorbance. A primary approach for controlling for formation of regulated DBPs, i.e. THMs and HAAs, is effective removal of NOM before disinfection, because aromatic fractions in NOM serve as the major precursors of THMs and HAAs (Gallard and von Gunten, 2002). However, AC moderately and even poorly removes DON and TDN in water, thereby leading to a high ratio of DON to DOC in the AC-treated water (Chiu et al., 2012), which may increase the ratios of N-DBPs to C-DBPs during the subsequent chlorination and chloramination (Chiu et al., 2012).

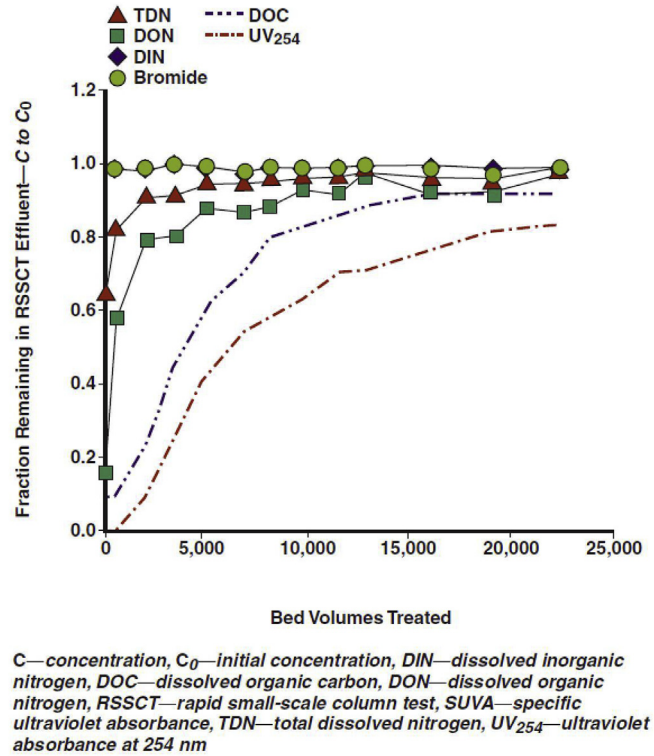

Fig. 2. Normalized DOC, UV_{254}, TDN, DIN, DON and Br^- breakthrough curves from RSSCTs conducted with sedimentation basin effluents. Adapted from Chiu et al. (2012).

Br^- is an almost inert constituent during AC adsorption. Consequently, the ratios of Br^- to DOC (Br^-/DOC) and Br^- to DON (Br^-/DON) in the GAC effluent significantly increase (Summers et al., 1993; Chiu et al., 2012). Moreover, the AC-treated water has a lower chlorine demand than the water without AC adsorption, thereby decreasing the ratio of free available chlorine (FAC) to Br^- (FAC/Br^-) after AC adsorption (Summers et al., 1993; Symons et al., 1993). Consequently, the increased Br^-/DOC and decreased FAC/Br^- favor the bromine incorporation into DBPs, increasing the ratio of Br-DBPs to Cl-DBPs (Symons et al., 1993; Krasner et al., 2016b; Zhang et al., 2017). To our knowledge, there are no relevant reference reported the ratio of bromine in Br-DBPs to TOX until now. This is a research gap and warrants to be investigated in future

Table 2
Effects of AC on the reaction of chlorinated oxidants with compounds absorbed onto the AC.

Precursors	Experimental conditions	Key finding	References
50 × 60 mesh HD 3000 (IC1 America Inc.)	Batch experiments: AC = 0.4 g/L, Cl_2 = 1.0 g/L, pH = 7.0 (initial) and time = 4 days.	GAC reacted with excess amount of free chlorine produced high molecular-weight brown-black colored products, smaller aromatic hydrocarbons and volatile chlorinated organic compounds.	Snoeyink et al., (1981)
50 × 60 mesh F-400 AC (Calgon Corp.)	Column experiments: 3 mm I.D. tube, AC = 0.5 g, Cl_2 = 10 −50 mg/L, pH = 8.0 (initial) and flow rate = 4.2 mL/min.	Brown-black colored products and volatile compounds were hardly observed in the effluents.	
16 × 20 mesh WV-G AC (Westvaco)	Column experiments: 3 cm I.D. tube, AC = 52.5 g, Cl_2 = 10 mg/L, pH = 5.6 (initial) and flow rate = 14.2 mL/min.		
30 × 40 mesh F-400 AC (Calgon Corp.)	Column experiments: 3 cm I.D. tube, AC = 52.5 g, Cl_2 = 10 mg/L, pH = 6.0 (initial) and flow rate = 14.2 mL/min.		
50 × 60 mesh F-400 AC (Calgon Corp.)	Batch experiments: AC = 0.4 g/L, NH_2Cl (as Cl_2) = 0.1 −1.0 g/L and pH = 7.0–8.0 (initial).	Monochloramine reacted much slower with GAC than free chlorine.	Chen et al., (1982)
8 × 16 mesh HD 300 (IC1 America Inc.)	Batch experiments: AC = 0.19 g/L and 0.041 g/L, ClO_2 = 95 −400 mg/L, pH = 3.5 (initial) and time = 3 weeks.	The formation of volatile organic compounds and the increase of TOX were not observed, whereas 22–37% of the chlorine dioxide was converted into chlorate.	
30 × 40 mesh HD 3000 (IC1 America Inc.)	Column experiments: 1.9 cm I.D. glass column, AC = 48.7 g, ClO_2 = 3.8 mg/L, pH = 3.5 (initial), hydraulic loading = 2.97 m/h and time = 4 days.	Formation of halogenated compounds, chlorate and the increase of TOX could be neglected from the chlorine dioxide-carbon reaction.	
Humic substances	Column experiments: 1.9 cm I.D. × 38 cm L. glass column, influent TOC = 9.2 mg/L, 30 × 40 mesh F-400 AC (Calgon Corp.) AC = 0.5 g, Cl_2 = 13.3 mg/L, pH = 6.3 (initial) and flow rate = 76.3 L/(m^2 × h). Column experiments: 1.9 cm I.D. × 38 cm L. glass column, influent TOC = 6.2 mg/L, AC = 0.5 g, Cl_2 = 8.1 mg/L, pH = 5.7 (initial) and flow rate = 76.3 L/(m^2 × h).	There was no substantial difference for products formed from the reaction of chlorine with adsorbed humic substances and formed from the chlorine reaction with humic substances in aqueous solution, excluding several dihydroxybenzenes and chlorinated dihydroxybenzenes.	McCreary and Snoeyink, (1981)
Resorcinol	N.A.	Reaction of resorcinol absorbed onto AC with free chlorine or chlorine dioxide formed significant chlororesorcinols and additional products, such as chlorinated cyclopentenediones.	Jackson et al., (1987)
Phenolic acids (p-hydroxybenzoic acid, vanillic acid and syringic acid)	Column experiments: 1.9 cm I.D. × 38 cm L. glass column, each of three precursors = 1.3 mg/L, 30 × 40 mesh F-400 AC (Calgon Corp.) = N.A., Cl_2 = 15.1 mg/L, pH = 6.0 (1 Mm phosphate buffer) and flow rate = 76.3 L/(m^2 × h).	Reaction of resorcinol absorbed onto AC with free chlorine or chlorine dioxide yielded additional products, such as polyphenols and quinones that were not produced by the reaction of chlorine in aqueous solution in the absence of carbon.	McCreary et al., (1982)
Substituted anilines	N.A.	Chlorination of substituted anilines absorbed onto AC yield several additional *N*-acylation, *N*-carbomethoxylation, *N*–*N* dimerization products and deamination and hydroxylation products.	Hwang et al., (1990)
Phenol, guaiaco, 2,6-dimethoxyphenol, catechol and *p*-chlorophenol	Column experiments: 1.9 cm I.D. × 2.0 cm L. glass column, 20 × 30 mesh F-400 AC (Calgon Corp.) = 2.3 g, precursor = 3.0 mg/L, Cl_2 = 8.0 mg/L, pH = 6.0 (1 Mm phosphate buffer) and hydraulic loading = 1.2 m/h. Column experiments: 1.0 cm I.D. × 5.0 cm L. glass column, 20 × 30 mesh F-400 AC (Calgon Corp.) = 1.6 g, precursor = 50 mg/L, Cl_2 = 10 mg/L, pH = 6.0 (1 Mm phosphate buffer) and hydraulic loading = 1.2 m/h.	Chlorination of phenols GAC absorbed onto AC yield several additional hydroxylation of the aromatic ring, oxidation products (quinones) and chlorine substitution, carboxylation, oxidative coupling products (dimers).	Voudrias et al., (1985a)
Hydrocarbons with benzylic hydrogen (ethylbenzene, indan, tetralin, diphenylmethane and fluorene)	Precursor = 0.5 mg/L, ClO_2 = 3–6 mg/L and pH = 3.5 (initial).	ClO_2 react readily with hydrocarbons with benzylic hydrogen to give oxidized derivatives such as ketones and alcohols, whereas some chlorinated compounds generated in the presence of GAC.	Chen et al., (1982)
Phenol and *p*-nitraophenol	Column experiments: 1.1 cm I.D. × 8.5 cm L. glass column, 12 × 40 mesh mineral-based GAC (CECA 40) = 3.0 g, precursor = 0 or 200 mg/L, Cl_2 = 0 or 50 mg/L, pH = 7.2 (5 Mm phosphate buffer), flow rate = 0.36 L/h and hydraulic loading = 3.7 m/h.	GAC promoted the reaction of chlorite with phenols to form chlorophenols, p-benzoquinone, dimerization, and carboxylation products, which were not produced from the chlorite-phenol reaction in aqueous solution.	Vel Leitner et al., (1994)

N.A., Not available.

study. Krasner et al. (2016b) reported that GAC treatment resulted in the greater genotoxicity in the presence of Br^- than an expected level, due to the formation of more Br-DBPs with stronger geno- and cytotoxicity. Therefore, though AC adsorption is an effective treatment option for controlling the formation of regulated C-DBPs through the abatement of NOM, it poorly prevents the formation of N-DBPs and Br-DBPs. Since N-DBPs are generally more cyto- and genotoxic than the regulated C-DBPs and Br-DBPs are generally more cyto- and genotoxic than their chlorinated analogs, additional treatments for the enhanced removal of Br^- and DON are needed before GAC treatment of influents with appreciable levels of Br^- (>~50 μg/L) and DON (>~0.3 mg-N/L) (Plewa et al., 2008; Plewa and Wagner, 2015). It should also be remembered that DBP FP is not equivalent to authentic DBP concentrations and increases in the relative proportions of particular groups of DBPs may still be accompanied by overall decreases in DBP concentrations.

When chlorine, chloramines or chlorine dioxide is used for pre-oxidation, their reactions with AC and adsorbed compounds onto AC inevitably occur (Table 2). The pre-treatment has been demonstrated to produce toxic byproducts and/or increase total organic halogen (TOX) concentrations, as shown in Table 2 (McCreary and Snoeyink, 1981; Chen et al., 1982; Voudrias et al.,

1985b; Stüber et al., 2005). Several chlorinated organic compounds and chlorate were found to be generated from the reactions of chlorine-containing disinfectant (i.e. free chlorine, monochloramine and chlorine dioxide) and AC (Snoeyink et al., 1981; Chen et al., 1982). However, it should be noted that the disinfectant doses used in the previous studies were much greater than those during realistic drinking water treatment. Recently, Zhang and colleagues also found similar phenomenon (Jiang et al., 2017, 2018). Therefore, the formation of sufficient undesirable DBPs from the reactions between these chlorine-containing disinfectants and AC in a treatment train is an unlikely concern (Snoeyink et al., 1981; Chen et al., 1982).

Previous efforts were made to explore the differences of final products between the reactions of disinfectants with NOM and with organic compound absorbed onto AC, as shown in Table 2 (McCreary and Snoeyink, 1981; Chen et al., 1982; McCreary et al., 1982; Chen et al., 1984; Voudrias et al., 1985b; a; Jackson et al., 1987; Hwang et al., 1990; Gonce and Voudrias, 1994; Vel Leitner et al., 1994). Many unwanted oxidation products are identified from the latter reaction pathway, including hydroxylation products, quinones, chlorine substitution products, carboxylation and oxidative coupling products (Chen et al., 1984). Of note, these compounds are typically more toxic than regulated DBPs (Du et al., 2013; Yang and Zhang, 2013; Liu and Zhang, 2014). However, the typical doses of chlorine-containing pre-oxidants (e.g. chlorine, chloramines or chlorine dioxide) applied during realistic disinfection are lower than 1 mg/L, much less than the oxidant doses selected in the laboratory studies (up to a few g/L). Moreover, because part of the oxidants has been scavenged by NOM in raw water during pre-oxidation, the real concentration of the oxidant can be further reduced before AC adsorption. Therefore, the reactions of residual chlorine-containing pre-oxidants with NOM absorbed onto AC cannot pose a serious threat in terms of the DBP formation.

2.4. Nanomaterials

Applications of various nanomaterials such as adsorbents, filter media, disinfectants, and reactive agents, have a potential to revolutionize the traditional treatment processes for the water treatment industry. For example, fullerene (C_{60}) has potential uses as an adsorbent in drinking water treatment and C_{60} is likely to be oxidized during chemical disinfection (Alpatova et al., 2013). A series of studies demonstrated that functionalized carbon nanotubes (CNTs) can be used as sorbents for organic pollutants, complexation agents for metals, and sensitizers for hydroxyl radical formation (Pan and Xing, 2008; Chen and Jafvert, 2010). However, the most studies on nanomaterial-based water treatment were carried out at a laboratory or pilot scale (Li et al., 2008; Tofighy and Mohammadi, 2011; Adeleye et al., 2016). Concerns about adoption of nanomaterials at full-scale water treatment facilities have been raised, including the regulatory challenges, technical hurdles, public perception, and uncertainties about fate of nanomaterials in the environment (Adeleye et al., 2016).

C_{60} can undergo surface reactions with ozone and chlorine in water and then be transformed into C_{60} derivatives containing hydroxyl, hemiketal and epoxy functional groups (Fortner et al., 2007; Wang et al., 2012). The transformation rate of C_{60} by photochlorination under the fluorescent light was much faster than that in the dark. Moreover, the presence of Cl atoms covalently bonded to C atoms has been confirmed by X-ray photoelectron spectroscopy peaks corresponding to a binding energy of 200.1–202.4 eV, indicating that C_{60} may be a precursor of DBPs (Wang et al., 2012; Alpatova et al., 2013). The specific DBP yields form C_{60} deserves a further investigation.

CNTs were reported to serve as the precursor of NAs and halogenated DBPs, including THMs, HAAs and HNMs (Verdugo et al., 2014, 2016). Concentrations of NDMA produced from the reactions of CNTs with free chlorine, monochloramine, and ozone were lower than those reported for those from the reactions with polymer coagulants. The NDMA yield reaches 50 ± 15 ng NDMA/mg CNTs (Verdugo et al., 2014). However, CNTs cannot make a significant contribution to the formation of NDMA, because the majority of NDMA from the chloramination, chlorination and ozonation of CNTs was lower than 10 ng NDMA/mg CNTs. Du et al. (2016) investigated the formation mechanisms and kinetics of THMs during the chlorination of five CNTs, graphene oxide (GO) and reduced GO. GO exhibited the greatest yield of THM derived from these nanomaterials, but the THM yield was only up to 1.0 μg TCM/mg GO after 120 h chlorination with 140 μM free chlorine. Therefore, CNTs seem not to be a major precursor of THMs in drinking water due to their low THM yields in comparison to that of NOM (Du et al., 2016).

In order to minimize the formation of regulated DBPs, alternative disinfection methods, including titanium dioxide photocatalysis (TiO_2/PC) and TiO_2 photoelectrocatalysis (TiO_2/PEC), are explored. Richardson et al. (1996) identified 3-methyl-2, 4-hexanedione as a DBP in an ultrafiltration membrane treated filtrate after the TiO_2/PC treatment. A number of DBPs, including Cl-DBPs, Br-DBPs and bromate, were also observed after the PEC treatment of HA in the presence of Cl^- or Br^- (Selcuk et al., 2006; Selcuk, 2010). Similar to other AOPs, HO• and other ROS generated in a TiO_2/PC system are capable of inactivating various microorganisms and destructing numerous organic and inorganic water contaminants, while generating certain DBPs (Richardson et al., 1996; Sokolowski et al., 2014). When chlorine is used after TiO_2/PC, both the increase and decrease of DBPFP in the treated water were reported, depending on the specific water characteristics (Li et al., 1996; Liu et al., 2008; Sokolowski et al., 2014). Metch et al. (2015) investigated the catalytic properties of silver nanoparticles (AgNPs), TiO_2, ceria and nano zero-valent iron (nZVI) on the formation of DBPs under disinfections with three different disinfection options, i.e. free chlorine, UV alone and UV/chlorine. Results showed that only AgNPs significantly promoted the formation of THMs during UV/chlorine (Metch et al., 2015). However, the same results were not found by Tugulea et al. (2014) under similar experimental conditions.

In summary, though the aforementioned nanomaterials may potentially contribute to the formation of regulated DBPs (i.e. THMs, HAAs and NAs) in drinking water, the role of these nanomaterials appears to be insignificant due to their typically low DBP yields in comparison to those of NOM. The potential environmental and health effects of these nanomaterials may be of real concern (Qu et al., 2013; Adeleye et al., 2016).

2.5. Ion-exchange resins

In drinking water treatment, ion exchange is the exchange of ions with the same charges between water and an insoluble solid (i.e. resins). Strong base ion-exchange resins are commonly used in the anion-exchange processes for the removal of negatively charged pollutants, such as nitrate, arsenate and perchlorate in raw water, because ion exchange technologies are simple, effective, selective, and relatively low-cost due to the repeated use after the resin regeneration (Gough et al., 1977; Samatya et al., 2006; Kemper et al., 2009). However, NDMA at a concentration of up to 2000 ng/L is found after ion exchange treatment of tap water or chlorinated water (Fiddler et al., 1977; Gough et al., 1977; Kimoto et al., 1980). NDMA is also observed in two samples of deionized water after ion exchange treatment (Fiddler et al., 1977), indicating that ion-

exchange resins may release organic compounds serving as the precursor of NDMA. Of interest, the presence of nitrite can double the formation of NDMA in a deionized water system placing these resins (Najm and Trussell, 2001). However, the aforementioned studies may have overestimated the NA formation, because the empty bed contact time used in these laboratory studies was much longer than that typically applied in the realistic full scale treatment plants.

Kemper et al. (2009) comprehensively evaluated the formation of NAs in anion-exchange column experiments with and without disinfection using free chlorine or chloramine before or after the resin columns. Results showed that the use of three commercially available strong base ion-exchange resins, including Rohm and Haas Amberlite IRA400, Sybron Ionac SR6 and Sybron Ionac ASB2, did not produce NAs at a concentration above the notification levels in the absence of disinfectants. When chlorination or chloramination followed ion exchange, the formation of NAs was not enhanced. However, upstream disinfection with chlor(am)ine significantly increased the TONO concentrations to 20–100 ng/L for the IRA400 and SR6 resins and to ~ 400 ng/L for the ASB2 resin, all above the California notification level (10 ng/L). These findings highlight that application of anion-exchange resins may be problematic due to the formation of certain DBPs. Moreover, when feed water with 2 mg/L chlorine passed through different ion exchange resins, the SR6 resin was the one with the greatest formation of TCNM (up to 9 μg/L). But the highest TCNM concentration (up to 10 μg/L) was observed in the sample of IRA400 during the treatment of water containing 2 mg/L NH_2Cl as Cl_2 (Kemper et al., 2009). When feed water without oxidation passed through the fresh ASB2 and IRA400 resins, traceable TCNM was observed in only one sample of the fresh IRA400 resin followed by chloramination (Kemper et al., 2009). Although the formation of TCNM is negligible without oxidation, concerns on the formation of unwanted DBPs remain.

To sum up, application of ion-exchange resins for direct treatment of tap water or chlorinated water needs to be cautious due to the potential formation of DBPs. Owing to recent efforts to produce new resin materials, research is required to investigate the contribution of new ion exchange resins to the formation of DBPs.

2.6. Membranes

Membrane filtration is a separation process that can separate two phases via a membrane material (Takht Ravanchi et al., 2009). In water treatment, the technology can remove particulate or dissolved pollutants such as NOM from water. The most common membrane separation processes in drinking water treatment are the pressure-driven membrane filtration, including microfiltration, uitrafiltration, nanofiltration (NF), and reverse osmosis (RO). Ersan et al. (2015) noticed that NDMA precursors could leach from five NF membranes and the NDMA FP of the permeate ranged within ~180–450 ng/L. Xie et al. (2015) also found that chlorination of polyvinyl pyrrolidone–polysulfone membranes led to the leaching of organic compounds from the membrane material and the formation of TCM, CH, TCNM, 1,1,1-trichloropropanone (1,1,1-TCP), and 1,1-dichloropropanone (1,1-DCP). Concentrations of these compounds reached a few μg/L. CH was the dominant by-product, followed by TCM, 1,1,1-TCP, 1,1-DCP and TCNM, in terms of their abundance. When chlorine dose was increased from 0 mg/L to 14.2 mg/L, the concentrations of TCM, CH and TCNM were increased to 5.2 μg/L, 12.4 μg/L and 0.8 μg/L. However, such high doses and long contact time (72 h) were rarely used in realistic drinking water treatment. Moreover, membrane separation units were typically applied in the upstream of disinfection. Furthermore, the aforementioned studies may have overestimated the DBP formation, because the long-time soaking used in these laboratory studies was not representative of membrane operation that typically applied in the realistic full scale treatment plants. Besides, the realistic leaching of organic compounds may be vary from lab studies because static pipe experiment used in these laboratory studies are different from that typically used in full-scale water supply. Static experiments may limit the continuous leaching of organic compounds when the chemical equilibrium of organic compounds is reached. Therefore, the leaching of membrane materials is not a major concern in the formation of halogenated DBPs when chlor(am)ination is applied after the membrane filtration. It should be noted that membrane cleaning with higher doses of chlorine may produce more halogenated DBPs, which may be a concern (Cai et al., 2017; Sun et al., 2018).

Furthermore, Chellam (2000) reported that NF could influence the speciation of DBPs in the downstream disinfection. Similar to GAC treatment, NF treatment can increase the molar ratio of Br-DBPs to Cl-DBPs in its permeate, even if chlorination of nanofiltered waters produced lower DBPs. They noticed that BCAA and TBAA accounted for 50% of the total HAAs on a molar basis as Br^-/DOC increased to 25 μM/mM or greater. It should be noted that the majority of HAAs produced are not regulated in existing five HAAs (HAA_5) regulations and guidelines. Bromine incorporation into THMs and HAAs was a function of [Br^-]/[DOC] that influences the speciation of DBPs produced. A model was further developed to correlate the bromine incorporation factors (BIFs) of THMs and HAAs with chlorination conditions as well as Br^- and DOC concentrations (Chellam, 2000). BIF is defined as the molar ratio of bromine incorporated into a given class of DBP to the total halogens in that class. It should be noted that BIF was typically increased after NF treatment, suggesting that chlorination following NF treatment potentially increased the mammalian cell cytotoxicity and genotoxicity, though the overall DBP concentrations may decrease. Particularly, HAA_9 concentrations were greater than the 4 regulated THMs (THM_4) level in the NF permeate (Chellam and Krasner, 2001; Chellam et al., 2008). According to CHO cell experiments, the toxicity of HAAs as a class is higher than THMs (Wagner and Plewa, 2017). Thus, a more equitable regulation of THMs and HAAs may be worthy of consideration.

Similar to AC treatment, treatment of high bromide-containing water using a membrane separation also promotes the ratio of brominated DBPs to chlorinated DBPs in effluents. Organic compounds leaching from membrane can bring about potential risks associated with the formation of DBPs during a downstream disinfection.

3. Unintended effects of engineering agents and materials in drinking water distribution on DBP formation

Drinking water distribution systems (DWDSs) are an essential component in municipal water supply. Iron, copper and zinc are widely incorporated into the materials in DWDSs and water storage facilities (Seidel, 1985). A 2004 survey of American Water Works Association (AWWA) indicates that iron based (i.e. ductile iron, cast iron and steel), PVC, and asbestos cement pipes account for 56.6%, 16.6% and 15.2% of total pipe miles, respectively (USEPA, 2007). Moreover, copper, polymer, lead, iron, and galvanized pipes are 56.3%, 19.6%, 3.3%, 2.7% and 8.0% of the total customer service lines, respectively (USEPA, 2007). Over the service time, the interior surface of metallic pipes exposed to an oxic environment is gradually corroded. Biofilms attached to the pipe walls are ubiquitous in DWDSs, contributing to more than 90% of the overall biomass (Flemming et al., 2002; Liu et al., 2016). However, only up to 5% of the biomass suspended in the bulk water can be monitored using the sampling procedure of drinking water. Therefore, microbial

Table 3
Experimental conditions and results for the reactions of DBPs with metal or metal corrosion products.

Metal specie	DBP specie	Compound	Reaction condition	Pseudo-first order rate constants (h^{-1})	References
Iron	HAAs	MCAA, MBAA, DCAA, BCAA, DBAA, TCAA, BDCAA, DBCAA, and TBAA	Iron = 0.5 g/L; initial pH = 3.9 ± 0.3; shaking velocity = 38 rpm; and room temperature.	N.S. - 1.41 ± 0.28	Hozalski et al., (2001)
		MCAA, MBAA, DCAA, BCAA, DBAA, TCAA, BDCAA, DBCAA, and TBAA	Iron = 2.4 g/L; pH = 7.5 buffered with 50 mM deoxygenated 3-morpholinopropanesulfonic acid (MOPS); shaking velocity = 45 rpm; and 25 °C.	8.16×10^{-4} - 19.65	Zhang et al., (2004)
		MCAA, DCAA, and TCAA	Iron = 0.55 g/L; DO = 1.52 mg/L; initial pH = 7.0; shaking velocity = 40 rpm; and room temperature.	$0.16 \pm 2.40 \times 10^{-3}$ - $0.67 \pm 1.44 \times 10^{-2}$	Tang et al., (2015)
		TBAA	New iron pipe; pH = 7.5 buffered with 50 mM deoxygenated MOPS; and room temperature.	$(6.00 \pm 1.00) \times 10^{-3}$ - $(3.73 \pm 2.25) \times 10^{-1}$	Arnold et al., (2010)
	HKs	1,1,1-trichloropropanone	Iron = 3.0 g/L; DO = 0 mg/L; pH = 7.5 buffered with 50 mM deoxygenated MOPS; shaking velocity = 50 rpm; and 20 ± 1 °C.	1.44 ± 0.12	Lee et al., (2007)
	HANs	TCAN	Iron = 3.0 g/L; DO = 0 mg/L; pH = 7.5 buffered with 50 mM deoxygenated MOPS; shaking velocity = 50 rpm; and 20 ± 1 °C.	1.38 ± 0.12	Lee et al., (2007)
	HNMs	Chloropicrin, DCNM, and MCNM	Iron = 1.8 g/L; pH = 7.5 buffered with 25 mM deoxygenated MOPS; shaking velocity = 45 rpm; and room temperature (23 °C).	1.02 ± 0.29–2.75 ± 0.42	Pearson et al., (2005)
	HAMs	TCAM, BDCAM, DBCAM, and TBAM	Iron = 10.0 g/L; copper = 11.4 g/L; pH = 6.0 buffered with Sodium acetate (0.1 M), 2-(N-morpholino) ethanesulfonic acid (MES) (0.03 M) and tris(hydroxymethy) aminomethane (Tris) (0.05 M); shaking velocity = 150 rpm; and 25 ± 0.2 °C.	N.A.	Chu et al., (2016a)
	NAs	NDMA	Iron column (50 cm × 3.81 cm ID); flow rate = 0.21 mL/min; unbuffered deionized water; room temperature	0.35 ± 0.05	Gui et al., (2000)
			Iron = 10 g/L; initial pH = 7.0; shaking velocity = 45 rpm; and 20 °C.	N.S.	Han et al., (2017)
	Inorganic DBPs	Bromate	Iron = 10 g/L; initial pH = 7.0; shaking velocity = 40 rpm; and 25 ± 1 °C.	7.06 ± 0.41	Tang et al., (2017)
Zinc	HAAs	MCAA, MBAA, DCAA, DBAA, TCAA, and TBAA	Zinc = 10 mg/L; unbuffered deionized water; shaking velocity = 150 rpm; and 25 ± 0.2 °C.	N.S. - 2.186	Wang and Zhu, (2010)
	NAs	NDMA	Zinc = 10 g/L; initial pH = 7.0; shaking velocity = 150 rpm; and 20 °C.	1.215 ± 0.171	Han et al., (2013)
			Zinc = 10 g/L; $Cu(OH)_2$ = 2.0 mM; initial pH = 7.0; shaking velocity = 45 rpm; and 20 °C.	6.289 ± 1.532	Han et al., (2017)
Copper	HAMs	TCAM, BDCAM, DBCAM, and TBAM	Copper = 10 g/L; pH = 6.0 buffered with Sodium acetate (0.1 M), MES (0.03 M) and Tris (0.05 M); shaking velocity = 150 rpm; and 25 ± 0.2 °C.	N.S.	Chu et al., (2016b)
Magnetite	HNMs	TCNM and DCNM	1 mM total Fe(II) or/and a mineral loading of 0.8 g/L; pH = 7.5 buffered with 25 mM deoxygenated MOPS; shaking velocity = 50 rpm; and room temperature (20 ± 1 °C).	0.02 ± 0.001–0.05 ± 0.01	Chun et al., (2005)
	HANs	TCAN		$(2.1 \pm 1.3) \times 10^{-3}$	
Fe(II)	HNMs	TCNM and DCNM		0.17 ± 0.01–3.63 ± 0.23	
	HANs	TCAN		$(8.2 \pm 1.0) \times 10^{-3}$	
Fe(II)/goethite	HNMs	TCNM and DCNM		1.13 ± 0.06–7.67 ± 0.44	
	HANs	TCAN		$(3.2 \pm 0.2) \times 10^{-2}$	
	HALs	TCAL (CH)		$(5.7 \pm 1.4) \times 10^{-4}$	
Fe(II)/magnetite	HNMs	TCNM and DCNM		1.22 ± 0.09–8.05 ± 0.67	
	HANs	TCAN		$(1.1 \pm 0.1) \times 10^{-2}$	
	HKs	1,1,1-TCP		$(0.9 \pm 0.4) \times 10^{-3}$	
	HALs	TCAL (CH)		$(1.3 \pm 0.9) \times 10^{-4}$	
Carbonate green rust ($GR(CO_3^{2-})$)	HAAs	MBAA, DCAA, DBAA, TCAA, and TBAA	2.4 g/L $GR(CO_3^{2-})$; pH = 7.5 buffered with 25 mM deoxygenated MOPS or 50 mM carbonate buffer; shaking	$(1.2 \pm 0.2) \times 10^{-3}$- 9.5 ± 1.48 (MOPS buffer); N.S. - 1.0 ± 0.08 (carbonate buffer)	Chun et al., (2007)

Table 3 (*continued*)

Metal specie	DBP specie	Compound	Reaction condition	Pseudo-first order rate constants (h^{-1})	References
	HKs	1,1,1-TCP	velocity = 50 rpm; and room temperature (22 ± 3 °C).	(3.9 ± 1.3) × 10^{-3} (MOPS buffer); N.S. (carbonate buffer)	
	HALs	TCAL (CH)		(2.2 ± 0.1) × 10^{-3} (MOPS buffer); N.S. (carbonate buffer)	
	HNMs	TCNM, DCNM, and MCNM		5.7 ± 1.03–55.2 ± 10.2 (MOPS buffer); 1.4 ± 0.01–32.5 ± 2.94 (carbonate buffer)	
	HANs	TCAN and DCAN		(8.1 ± 0.7) × 10^{-3}- 0.9 ± 0.08 (MOPS buffer); N.S. – 0.17 ± 0.03 (carbonate buffer)	
Iron pipe corrosion solids	HNMs	TCNM	Pipe solids = 2.5 g/L; pH = 7.5 buffered with 25 mM deoxygenated MOPS; shaking velocity = 50 rpm; and room temperature (20 ± 1 °C).	9 ± 1.2–68.4 ± 4.8	Lee et al., (2008)

N.S. Not significant; N.A. Not available; C = chloro, B = bromo, I = iodo, T = tri, D = di, M = mono; Errors represent 95% confidence limits.

contamination in the pipes is underestimated (Flemming et al., 2002). Previous studies have revealed that the occurrence of biofilms within the pipes can accelerate depletion of disinfectant residual, favor excessive accumulation of microorganisms, increase the release of pipe corrosion products, decrease water pH, and lower dissolved oxygen (DO) (Emde et al., 1992; Lehtola et al., 2004; Zeng and Mitch, 2016). Kinetics and mechanism of these reactions of disinfectant residuals with NOM, pipe deposits and pipe biofilms may play an essential role in the fate and transportation of DBPs within DWDSs. Moreover, hydraulics patterns, seasonal variables and the finished water quality all impact the fate and transportation of DBPs within DWDSs.

3.1. Distribution system pipes

Based on the AWWA's Water://Stats database in 2002, 22.5% of 202158-mile U.S. DWDSs are made of unlined cast/ductile iron or steel (USEPA, 2007). It is well known that elemental transition metals, such as iron, zinc and copper, are commonly used as reductants to detoxify halogenated organic compounds in site remediation (Matheson and Tratnyek, 1994; Arnold and Roberts, 1998). To understand the fate of DBPs in DWDSs and to develop possible treatment processes for removal of DBPs from drinking water, numerous studies have focused on degradation of representative DBPs (i.e. THMs, HAAs, HALs, HKs, HANs, HNMs, HAMs and NAs) in the presence of zero-valent metals (Gui et al., 2000; Hozalski et al., 2001; Zhang et al., 2004; Pearson et al., 2005; Lee et al., 2007; Arnold et al., 2010; Wang and Zhu, 2010; Han et al., 2013, 2017; Tang et al., 2015; Chu et al., 2016c). Table 3 presents the experimental conditions and results for the reactions of DBPs with different elemental metals. The metals, regardless of their shape and size, are capable of degrading halogenated DBPs and non-halogenated NAs via reductive mechanisms. Tendency of dehalogenation from the alkyl carbon decreases in the following order: I > Br ≫ Cl, due to an increasing bond length and a decreasing dissociation energy. Therefore, a faster dehalogenation rate occurs for I-DBPs than those of Br- and Cl-DBPs (Chu et al., 2016c). Moreover, the removal of Cl-DBPs initially increases and then decreases with the increase of DO (Lee et al., 2007; Tang et al., 2015). This finding can be explained by the theory that the degradation of Cl-DBPs is limited by the reduction or migration rate within metal particles rather than mass transfer (Zhang et al., 2004). In the iron-based pipes, low oxic condition favors the formation of a thin lepidocrocite layer, which can enhance the degradation of Cl-DBPs. In contrast, at a high oxic condition, oxygen competing for reductive agents and significant growth of lepidocrocite can inhibit reductive dehalogenation (Tang et al., 2015). Although the base-catalyzed hydrolysis of HAN, HAMs, HNMs, or HALs simultaneously occurred during the reduction process, the hydrolysis rates under typical drinking water conditions (pHs 7–8) were several orders of magnitude slower than that reduction reaction (Joo and Mitch, 2007; Yu and Reckhow, 2015; Ma et al., 2016; Ding et al., 2018c). Therefore, the effect of hydrolysis on the degradation of N-DBPs was not discussed in this study.

Although ZVI can theoretically remove many halogenated DBPs and NAs, the treatment efficiency of ZVI is discounted at realistic treatment condition. As shown in Table 3, the highest observed order degradation rate constant of halogenated DBPs and NAs under neutral condition reaches 19.65 h^{-1}, whereas the most observed rate constants are lower than 0.1 h^{-1}. Half-lives of the halogenated DBPs and NAs are more than several hours. In general, the dehalogenation tendency of halogenated DBPs decreases in the following order: I > Br ≫ Cl. Moreover, dehalogenation rates increase with the number of halogens substituted on the methyl group and monohalogenated DBPs are difficult to form non-halogenated compounds by dehalogenation. Furthermore, the corrosion products and biofilm also inhibit the dehalogenation reactions. Besides, DWDSs are composed of metal pipe rather than metal powder, and the surface area of metal pipe were several order lower than that of metal powder. Therefore, ZVI rarely completely degrades halogenated DBPs into non-halogenated compounds during the drinking water distribution. Although the observed rate constants for the reaction of zero-valent zinc with halogenated DBPs or NAs are usually higher than 1 h^{-1} (Table 3), zinc pipes are much less popularly used than iron based pipes.

While zero-valent metals (i.e. iron, zinc and copper) can serve as potential reductants capable of reducing a wide variety of halogenated DBPs and NAs, they were reported to enhance the formation DBPs or generate more toxic DBPs during water treatment. Chu et al. (2016a) demonstrated that the reduction of three chloramphenicol antibiotics by ZVI can produce DCAM firstly and then MCAM in the absence of disinfectants. Given that unlined cast iron pipes are widely used in many drinking water distribution systems, reactions between chloramphenicol antibiotics and ZVI may contribute to the formation of DCAM. I^- is considered as the main iodine source accounting for the formation of toxic I-DBPs during disinfection, while iodinated X-ray contrast media and iodate can also serve as the iodine sources of I-DBPs in the presence of ZVI (Xia et al., 2017; Dong et al., 2018). Iopamidol or iodate is subjected to the deiodination or reduction by ZVI to yield I^-, which enhances the formation of I-DBPs during subsequent chlor(am)ination (Xia et al., 2017; Dong et al., 2018). However, these reactions will also be inhibited by the aforementioned inhibiting factors for the zero-valent metal facilitated dehalogenation.

Polyvinyl chloride (PVC) and chlorinated PVC pipes may leach vinyl chloride, a confirmed human carcinogen, in several tens of ng/L over a couple of days and a few hundreds of ng/L after two-year exposure (Ando and Sayato, 1984; Benfenati et al., 1991; Walter et al., 2011). Results also demonstrated that aging had no significant effect on the accumulation of vinyl chloride (Walter et al., 2011). Although these levels exceed the maximum contaminant level goal of vinyl chloride at 0 μg/L in water, they are still much lower than that the EPA's maximum contaminant level of 2 μg/L (Walter et al., 2011). Nevertheless, similar to the leaching of membrane, the accumulation of vinyl chloride may be limited in static pipe experiment used in these laboratory studies. Morran et al. (2011) noticed that NDMA could not be generated from the reactions of PVC pipe with chloramine. However, a 24 h immersion of new rubber pipeline sealing rings, gate value inserts and gaskets, which are used to connect pipes and construct temporary storage tanks in ultrapure water, can cause the formation of NDMA ranging from <3 ng/L to 930 ng/L (Morran et al., 2011; Teefy et al., 2014). Furthermore, the presence of chlorine or chloramines produces 2-fold NDMA or greater under the identical conditions. Therefore, pre-treatments of these new rubber materials are of importance for alleviation of the NDMA formation.

In summary, the use of plastic and rubber, rather than metal, pipelines can become the major concern for serving as the source of NDMA.

3.2. Distribution system deposits

Corrosion products of iron pipes are comprised of various iron (hydr)oxides. Lin et al. (2001) identified goethite (75.6%), magnetite (21.5%) and lepidocrocite (2.9%) in complex iron corrosion products. Table 3 presents the degradation of DBPs in the presence of various synthetic and realistic pipe deposits. The dehalogenation rates of TCNM, TCAN, 1,1,1-TCP, CH, TCAA and CF, which share the same chemical structure CCl_3-R, increase with the increasing electron-withdrawal of substituents (-NO_2 > −CN > −C(=O)CH_3 > −CHO > -COO^- > −H) (Chun et al., 2005). This observation can be explained by the fact that electron-withdrawal groups can move electron density away from the -CCl_3 moiety, thereby becoming more electrophilic (Croue and Reckhow, 1989).

Although pipe deposits are capable of removing DBPs, half-lives of the DBPs are typically as long as several hours or greater (Table 3). Generally, dihalogenated and monohalogenated DBPs are more difficultly degradated than trihalogenated DBPs (Chun et al., 2005; Chu et al., 2016c). One previous study also reported that lead oxide (PbO_2) can oxidize iodide to reactive iodine, which lead to IF formation in the presence of NOM (Lin et al., 2008). However, the high oxidant and iodide doses and reaction time in that study hardly occurs in realistic DWDSs. Apart from reductive capability of the pipe deposits, they can serve as a catalyst for altering the decay rate of disinfectant and/or influencing the formation of DBPs (Blatchley et al., 2003; Chu et al., 2016c; Sharma et al., 2017). Catalytic effects of iron corrosion products on disinfectant decomposition are insignificant (Liu et al., 2013a; b; Zhao et al., 2016). However, copper corrosion products (CCPs), including Cu(II), Cu_2O, CuO and $Cu_2(OH)_2CO_3$, can accelerate the decay of oxidants, including HOCl, ClO_2, HOBr and HOI (Fig. 3) (Liu et al., 2012, 2014, 2013b). Along with the rapid decay of disinfectants in the presence of CCPs, the formation of THMs, HAAs, bromate, chlorate, chlorite and NAs in simulated DWDSs is enhanced (Li et al., 2007; Fu et al., 2009; Zhang and Andrews, 2012, 2013; Liu et al., 2013c; Zhao et al., 2016). Moreover, more TOX is produced during chlorination of drinking water in the presence of CCPs (Liu et al., 2013c). Fu et al. (2009) proposed two plausible pathways to explain the reaction mechanisms for the CCPs-catalyzed formation of THM and HAA. In

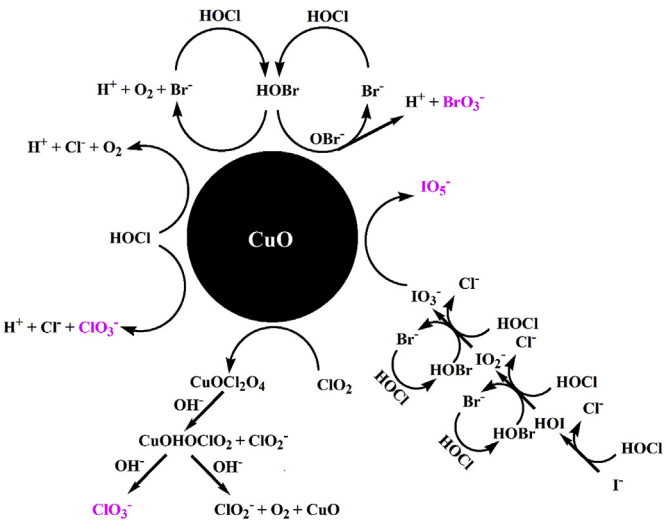

Fig. 3. Proposed reactions for CuO-enhanced HOCl, HOBr, HOI and ClO_2 decay. Adapted from Liu et al. (2012), Liu et al. (2013b) and Liu et al. (2014). The compounds labeled with red represented the enhanced products in the presence of CuO.

the first mechanism, the enhancement is attributed to the increased yield of •OH validated from the electron spin resonance analysis (Fu et al., 2009). A previous study also found that metal-loaded HA could produce •OH through the metal-driven Fenton chemistry (Paciolla et al., 1999). •OH is capable of oxidizing large molecular weight (MW) NOM compounds (e.g. HA) into small MW molecules that are more reactive DBP precursors than the initial material (Hua and Reckhow, 2007). In the other pathway, CCPs complexes with HA can accelerate the decarboxylation steps for THM and HAA formation (Fu et al., 2009).

As shown in Fig. 3, CCPs also catalyze the disproportionation of HOBr to enhance the formation of bromate during chlorination of bromide-containing waters (Liu et al., 2012, 2013a). Subsequent studies indicated that the formation of bromate from the disproportionation of HOBr competed with the formation of Br-DBPs (Liu and Croué, 2016). Fractions of the product species rely on how reactively bromine reacts with NOM and how rapid HOBr disproportionation is. Results indicated that the reactivity of HOBr with phenols was much stronger than that of the HOBr disproportionation in the presence of CuO, whereas the disproportionation of HOBr prevails in comparison with the reactions of HOBr with certain less reactive compounds, such as acetone, butanol, propionic and butyric acids (Liu and Croué, 2016). Hu et al. (2016) reported that three CCPs (i.e. Cu(II), Cu_2O and CuO) simultaneously enhanced the formation of bromate and Br-DBPs during chlorination of bromide-containing waters. As shown in Fig. 4, 0.04% and 24.6% of Br^- (on a molar basis) are converted to bromate and Br-DBPs, respectively, in the absence of CCPs. However, the conversion ratios of Br^- to bromate rise to 22.1%, 8.6% and 9.1% in the presence of CuO, Cu_2O and Cu(II), respectively. Meanwhile, the conversion ratios of Br^- to the studied Br-DBPs reach 24.7%, 36.0% and 30.6%, respectively. It should be noted that there is a substantial discrepancy between Br^- with and without the addition of CCPs. The concentration of unutilized Br^- accounts for 23.9% of initial Br^- concentration in the absence of CCPs, while the unutilized Br^- decreases to 14.3%, 8.4% and 9.6% in the presence of CuO, Cu_2O and Cu(II), respectively. Furthermore, CuO, Cu_2O and Cu(II) catalyze the transformations of Cl-DBPs to brominated analogues in the presence of Br^- (Li et al., 2007; Liu et al., 2013a). It was reported that the concentrations of bromate and Br-DBPs (i.e. THMs, HAAs and HAMs) under CuO, Cu_2O or Cu(II) catalysis were generally lower

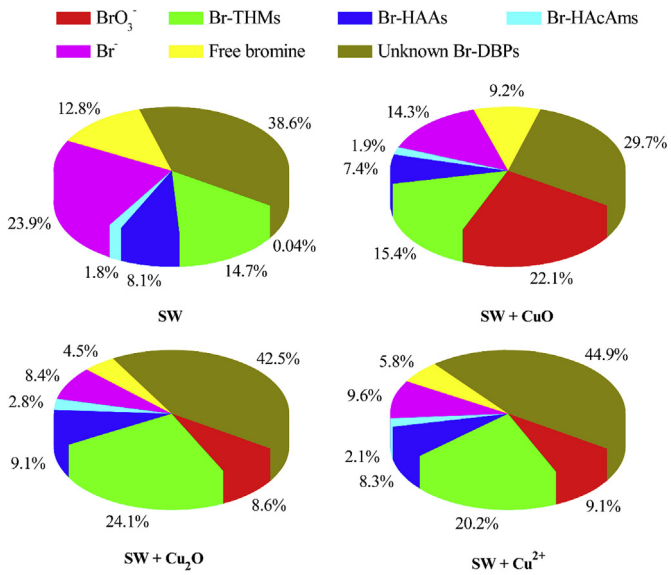

Fig. 4. Bromine mass balance in the presence of CCPs and HA during chlorination of synthetic water (SW). Experimental conditions: $Cl_2 = 14.2$ mg/L, $[Br^-]_0 = 2.0$ mg/L, $[HA]_0 = 5.0$ mg/L, $[CuO]_0 = 2.0$ g/L, $[Cu_2O]_0 = 0.5$ g/L, $[Cu^{2+}]_0 = 2.0$ mg/L, pH = 7.6, reaction time = 72 h. Adapted from the Hu et al. (2016).

than the maximum contaminant level at the Br^- concentration of 0.2 mg/L (Hu et al., 2016). However, when the Br^- concentration increased to 0.5 mg/L, the concentration of bromate after the CuO, Cu_2O or Cu(II) catalysis significantly increased, ranging from 15.1 to 54.6 μg/L, and the enhancement ratios of Br-DBPs (i.e. THMs, HAAs and HAMs) formation under Cu_2O catalysis were 47.4%, 44.0% and 42.9%, respectively, corresponding to 117.1 μg/L, 82.3 μg/L and 68.6 μg/L, all above or equivalent to their respective EPA's maximum contaminant levels (10 μg/L, 80 μg/L and 60 μg/L for bromate, THM_4 and HAA_5) (USEPA, 2006). Because Br-DBPs are generally more toxic than Cl-DBPs, the health risks associated with Br-DBPs should be paid special attention to when copper is used as the inlet pipe materials and the filter waters have higher Br^- level (>200 μg/L).

Accordingly, CCPs accelerate the decay of disinfectants, promote the formation of DBPs and total organic halogen, and lead to additional byproduct formation. A partial loss of disinfectants is problematic to drinking water quality and enhances formation of DBPs.

3.3. Distribution system biofilms

Numerous models have been developed to predict the formation of DBPs during water treatment, but the role of biofilms (up to 10^4–10^7 CFU/cm^2)) in these models has been generally underestimated (Ged et al., 2015; Abokifa et al., 2016). Similarly, the formation of DBPs in the DWDS environment is generally underemphasized (Rossman et al., 2001). Moreover, the concentration of THMs at DWDSs and the points of use are higher than those in finished water, while chlorine is rapidly consumed within the pipe system (Toroz and Uyak, 2005; Pieri et al., 2014). These findings show that DWDS pipe biofilms may have been an important DBP precursor.

Rossman et al. (2001) compared the formation of THMs and HAAs in a simulated DWDS pipe to that in a bottle. They found that the decline of chlorine was faster while the concentration of THMs increased by an average of 15% in simulated DWDS pipe. Moreover, the hydrolysis and chlorination of intermediate DBPs into THMs may also contribute to increases in the latter group and will be affected by pH values of the particular system. Many DBPs, including THMs, HALs, HKs, HNMs and HANs, are detectable at several tens μg/L regulated DBPs/mg-C/L or several μg/L N-DBPs/mg-C/L during chlor(am)ination of pure bacterial cells and EPS isolated from biofilms (Wang et al., 2013; Lemus Pérez and Rodríguez Susa, 2017). DBP FP is also correlated with the log reduction of bacterial cells (i.e. bacterial cells) and EPS (Wang et al., 2013; Lemus Pérez and Rodríguez Susa, 2017). Abokifa et al. (2016) developed a multiple species reactive transport model to predict chlorine decay and microbial regrowth dynamics in a realistic DWDS, along with THMs formation in a pilot-scale distribution system simulator by accounting for the simultaneous transport and interactions of disinfectants, organic compounds and biomass. Results indicate that the contribution of biofilm to the formation of THMs relies heavily on hydraulics patterns, seasonal variables and the finished water quality in the system (Abokifa et al., 2016). Besides, nitrification in storage facilities enhances the formation of NDMA and other halogenated DBPs in the downstream chloramine application in the DWDSs (Zeng and Mitch, 2016). The enhanced DBP formation in the presence of nitrifying biofilm indicates that the release of organic compounds from nitrifying biofilm can serve as the precursors of DBPs (Zeng and Mitch, 2016). An integrated approach, starting from the treatment of drinking water prior to entering the DWDSs to the potential implementation of "biofilm-limiting" operational conditions and, finally, ending with the careful selection of flushing of DWDS, nutrient removal, and emerging available technologies for biofilm monitoring and control, is needed.

Pipe biofilms accelerate coliform growth and pipe corrosion, lead to water taste and odour issues, and promote the decay of disinfectant and formation of DBPs. Therefore, appropriate management of biofilm growth in a water distribution system is of importance to the additional formation of DBPs within the pipes (Liu et al., 2016).

4. Conclusions and implications for drinking water treatment and distribution

Drinking water disinfection requires tradeoffs between the inactivation of pathogens and the formation of hazardous DBPs. This article reviews and analyses the unintended effects of engineering materials and reagents during drinking water treatment and distribution on the formation of DBPs. Quaternary ammonium polymer coagulants may lead to violation of the NDMA notification levels, which may be a major concern for the drinking water quality. Organic compounds leached from strong base ion-exchange resins, membranes and pipes can also cause noncompliance with regulatory limits. Biofilm formation in BAF and DWDSs can accelerate disinfectant decomposition and DBP formation. In order to minimize the biofilm facilitated formation of DBPs, it is essential to implement 'biofilm-limiting' operation, flush distribution systems and remove nutrients within the distribution system. Furthermore, the treatment of high Br^- (>~100 μg/L) source waters with AC or membranes can elevate toxicity in effluents, despite an overall decrease in the overall DBP concentrations. CCPs can accelerate the decay of disinfectants and oxidants, promote the formation of DBPs (particularly bromate), increase the concentration of TOX and lead to the formation of additional byproducts. A partial loss of disinfectants is problematic to drinking water quality and enhanced formation of DBPs makes this even worse. These impacts can be mitigated by replacement of copper pipes, application of lined cast copper pipes, flushing of distribution systems and improved monitoring of CCPs. This study highlights the role of engineering agents and materials in the formation of DBPs in water treatment and distribution.

Acknowledgements

The authors gratefully acknowledge the National Natural Science Foundation of China (No. 51822808; 51578389; 51778445), the National Major Science and Technology Project of China (No. 2017ZX07201-005), the Shanghai City Youth Science and Technology Star Project (No. 17QA1404400), Shanghai City Youth Top Talent Project and Fundamental Research Funds for the Central Universities (1380219169). S. Ding was partially supported by Shanghai Tongji Gao Tingyao Environmental Science & Technology Development Foundation (STGEF).

References

Abokifa, A.A., Yang, Y.J., Lo, C.S., Biswas, P., 2016. Investigating the role of biofilms in trihalomethane formation in water distribution systems with a multicomponent model. Water Res. 104, 208–219.
Adeleye, A.S., Conway, J.R., Garner, K., Huang, Y., Su, Y., Keller, A.A., 2016. Engineered nanomaterials for water treatment and remediation: costs, benefits, and applicability. Chem. Eng. J. 286, 640–662.
Alpatova, A.L., Baumann, M.J., Davies, S.H., Masten, S.J., 2013. Evidence for covalently bonded chlorine–fullerene formed by ozonation and chlorination at room temperature. Environ. Chem. Lett. 11 (3), 309–313.
Ando, M., Sayato, Y., 1984. Studies on vinyl chloride migrating into drinking water from polyvinyl chloride pipe and reaction between vinyl chloride and chlorine. Water Res. 18 (3), 315–318.
Arnold, W.A., Roberts, A.L., 1998. Pathways of chlorinated ethylene and chlorinated acetylene reaction with Zn(0). Environ. Sci. Technol. 32 (19), 3017–3025.
Arnold, W.A., Hozalski, R.M., Pearson, C.R., Morre, K., 2010. TBAA reduction in reactors simulating distribution system pipes. J. Am. Water Work. Assoc. 102 (3), 99–106.
Bablon, G.P., Ventresque, C., Aïm, R.B., 1988. Developing a sand-GAC filter to achieve high-rate biological filtration. J. Am. Water Work. Assoc. 80 (12), 47–53.
Bei, E., Shu, Y., Li, S., Liao, X., Wang, J., Zhang, X., Chen, C., Krasner, S., 2016. Occurrence of nitrosamines and their precursors in drinking water systems around mainland China. Water Res. 98, 168–175.
Benfenati, E., Natangelo, M., Davoli, E., Fanelli, R., 1991. Migration of vinyl chloride into PVC-bottled drinking-water assessed by gas chromatography-mass spectrometry. Food Chem. Toxicol. 29 (2), 131–134.
Blatchley, E.R., Margetas, D., Duggirala, R., 2003. Copper catalysis in chloroform formation during water chlorination. Water Res. 37 (18), 4385–4394.
Bolto, B., 2005. Reaction of chlorine with organic polyelectrolytes in water treatment: a review. J. Water Supply: Res. Teach. 54 (8), 531–544.
Bolto, B., Gregory, J., 2007. Organic polyelectrolytes in water treatment. Water Res. 41 (11), 2301–2324.
Bond, T., Huang, J., Templeton, M.R., Graham, N., 2011. Occurrence and control of nitrogenous disinfection by-products in drinking water – a review. Water Res. 45 (15), 4341–4354.
Bond, T., Templeton, M.R., Graham, N., 2012. Precursors of nitrogenous disinfection by-products in drinking water––A critical review and analysis. J. Hazard Mater. 235–236, 1–16.
Cai, W., Liu, J., Zhu, X., Zhang, X., Liu, Y., 2017. Fate of dissolved organic matter and byproducts generated from on-line chemical cleaning with sodium hypochlorite in MBR. Chem. Eng. J. 323, 233–242.
CDPH, 2009. NDMA and Other Nitrosamines e Drinking Water Issues. http://www.cdph.ca.gov/certlic/drinkingwater/Pages/NDMA.aspx.
Chellam, S., 2000. Effects of nanofiltration on trihalomethane and haloacetic acid precursor removal and speciation in waters containing low concentrations of bromide ion. Environ. Sci. Technol. 34 (9), 1813–1820.
Chellam, S., Krasner, S.W., 2001. Disinfection byproduct relationships and speciation in chlorinated nanofiltered waters. Environ. Sci. Technol. 35 (19), 3988–3999.
Chellam, S., Sharma, R.R., Shetty, G.R., Wei, Y., 2008. Nanofiltration of pretreated Lake Houston water: disinfection by-product speciation, relationships, and control. Separ. Purif. Technol. 64 (2), 160–169.
Chen, A.S.C., Larson, R.A., Snoeyink, V.L., 1982. Reactions of chlorine dioxide with hydrocarbons: effects of activated carbon. Environ. Sci. Technol. 16 (5), 268–273.
Chen, A.S.C., Larson, R.A., Snoeyink, V.L., 1984. Importance of surface free radicals in an aqueous chlorination reaction (Indan-ClO2) promoted by granular activated carbon. Carbon 22 (1), 63–75.
Chen, C.-Y., Jafvert, C.T., 2010. Photoreactivity of carboxylated single-walled carbon nanotubes in sunlight: reactive oxygen species production in water. Environ. Sci. Technol. 44 (17), 6674–6679.
Child, P., Kaa, G., Benitz, D., Fowlie, P., Hong, R., 1996. Reaction between Chlorine and a Dimethylamine Containing Polyelectrolyte Leading to the Formation of N-Nitrosodimethylamine.
Chiu, C.A., Westerhoff, P., Ghosh, A., 2012. GAC removal of organic nitrogen and other DBP precursors. J. Am. Water Work. Assoc. 104 (7), 406–415.
Chu, W.H., Gao, N.Y., Deng, Y., Krasner, S.W., 2010. Precursors of dichloroacetamide, an emerging nitrogenous DBP formed during chlorination or chloramination. Environ. Sci. Technol. 44 (10), 3908–3912.
Chu, W.H., Gao, N.Y., Deng, Y., Templeton, M.R., Yin, D.Q., 2011. Impacts of drinking water pretreatments on the formation of nitrogenous disinfection by-products. Bioresour. Technol. 102 (24), 11161–11166.
Chu, W.H., Li, C.J., Gao, N.Y., Templeton, M.R., Zhang, Y.S., 2015a. Terminating pre-ozonation prior to biological activated carbon filtration results in increased formation of nitrogenous disinfection by-products upon subsequent chlorination. Chemosphere 121, 33–38.
Chu, W.H., Li, D.M., Gao, N.Y., Yin, D.Q., Zhang, Y.S., Zhu, Y.P., 2015b. Comparison of free amino acids and short oligopeptides for the formation of trihalomethanes and haloacetonitriles during chlorination: effect of peptide bond and pre-oxidation. Chem. Eng. J. 281, 623–631.
Chu, W.H., Ding, S.K., Bond, T., Gao, N.Y., Yin, D.Q., Xu, B., Cao, Z.Q., 2016a. Zero valent iron produces dichloroacetamide from chloramphenicol antibiotics in the absence of chlorine and chloramines. Water Res. 104, 254–261.
Chu, W.H., Krasner, S.W., Gao, N.Y., Templeton, M.R., Yin, D.Q., 2016b. Contribution of the antibiotic chloramphenicol and its analogues as precursors of dichloroacetamide and other disinfection byproducts in drinking water. Environ. Sci. Technol. 50 (1), 388–396.
Chu, W.H., Li, X., Bond, T., Gao, N.Y., Bin, X., Wang, Q.F., Ding, S.K., 2016c. Copper increases reductive dehalogenation of haloacetamides by zero-valent iron in drinking water: reduction efficiency and integrated toxicity risk. Water Res. 107, 141–150.
Chuang, Y.-H., Mitch, W.A., 2017. Effect of ozonation and biological activated carbon treatment of wastewater effluents on formation of N-nitrosamines and halogenated disinfection byproducts. Environ. Sci. Technol. 51 (4), 2329–2338.
Chuang, Y.-H., Szczuka, A., Shabani, F., Munoz, J., Aflaki, R., Hammond, S.D., Mitch, W.A., 2019. Pilot-scale comparison of microfiltration/reverse osmosis and ozone/biological activated carbon with UV/hydrogen peroxide or UV/free chlorine AOP treatment for controlling disinfection byproducts during wastewater reuse. Water Res. 152, 215–225.
Chun, C.L., Hozalski, R.M., Arnold, W.A., 2005. Degradation of drinking water disinfection byproducts by synthetic goethite and magnetite. Environ. Sci. Technol. 39 (21), 8525–8532.
Chun, C.L., Hozalski, R.M., Arnold, W.A., 2007. Degradation of disinfection byproducts by carbonate green rust. Environ. Sci. Technol. 41 (5), 1615–1621.
Cornwell, D.A., Brown, R.A., Krasner, S.W., 2017. Evaluating polymers to avoid polymer-induced N-Nitrosodimethylamine formation. J. Am. Water. Works. Ass. 109 (6), E197–E214.
Croue, J.P., Reckhow, D.A., 1989. Destruction of chlorination byproducts with sulfite. Environ. Sci. Technol. 23 (11), 1412–1419.
Deborde, M., von Gunten, U., 2008. Reactions of chlorine with inorganic and organic compounds during water treatment—kinetics and mechanisms: a critical review. Water Res. 42 (1–2), 13–51.
Ding, S.K., Chu, W.H., Bond, T., Cao, Z.Q., Xu, B., Gao, N.Y., 2018a. Contribution of amide-based coagulant polyacrylamide as precursors of haloacetamides and other disinfection by-products. Chem. Eng. J. 350, 356–363.
Ding, S.K., Chu, W.H., Bond, T., Wang, Q., Gao, N.Y., Xu, B., Du, E.D., 2018b. Formation and estimated toxicity of trihalomethanes, haloacetonitriles, and haloacetamides from the chlor(am)ination of acetaminophen. J. Hazard Mater. 341, 112–119.
Ding, S.K., Chu, W.H., Krasner, S.W., Yu, Y., Fang, C., Xu, B., Gao, N.Y., 2018c. The stability of chlorinated, brominated, and iodinated haloacetamides in drinking water. Water Res. 142, 490–500.
Dong, H., Qiang, Z., Lian, J., Li, J., Yu, J., Qu, J., 2018. Deiodination of iopamidol by zero valent iron (ZVI) enhances formation of iodinated disinfection by-products during chloramination. Water Res. 129, 319–326.
Du, H., Li, J., Moe, B., McGuigan, C.F., Shen, S., Li, X.-F., 2013. Cytotoxicity and oxidative damage induced by halobenzoquinones to T24 bladder cancer cells. Environ. Sci. Technol. 47 (6), 2823–2830.
Du, T., Wang, Y., Yang, X., Wang, W., Guo, H., Xiong, X., Gao, R., Wuli, X., Adeleye, A.S., Li, Y., 2016. Mechanisms and kinetics study on the trihalomethanes formation with carbon nanoparticle precursors. Chemosphere 154, 391–397.
Emde, K.M.E., Smith, D.W., Facey, R., 1992. Initial investigation of microbially influenced corrosion (MIC) in a low temperature water distribution system. Water Res. 26 (2), 169–175.
Ersan, M.S., Ladner, D.A., Karanfil, T., 2015. N-nitrosodimethylamine (NDMA) precursors leach from nanofiltration membranes. Environ. Sci. Technol. Lett. 2 (3), 66–69.
Feige, M.A., Glick, E.M., Munch, J.W., Munch, D.J., Noschang, R.L., Brass, H.J., 1980. In: Jolley, R.L., Brungs, W.A., Cumming, R.B., Jacobs, V.A. (Eds.), Water Chlorination: Environmental Impact and Health Effects. Ann Arbor Science Publishers, Ann Arbor, Michigan, pp. 789–799.
Fiddler, W., Pensabene, J.W., Doerr, R.C., Dooley, C.J., 1977. The presence of dimethyl- and diethyl-nitrosamines in deionized water. Food Cosmet. Toxicol. 15 (5), 441–443.
Fielding, M., Hutchison, J., Hughes, D.M., Glaze, W.H., Weinberg, H.S., 1999. Analytical Methods for Polymers and Their Oxidative by-Products. AWWA Research Foundation, Denver, Colorado.
Flemming, H.C., Percival, S.L., Walker, J.T., 2002. Contamination potential of biofilms in water distribution systems. Water Sci. Technol. 2 (1), 271.
Fortner, J.D., Kim, D.-I., Boyd, A.M., Falkner, J.C., Moran, S., Colvin, V.L., Hughes, J.B., Kim, J.-H., 2007. Reaction of water-stable C60 aggregates with ozone. Environ. Sci. Technol. 41 (21), 7497–7502.
Fu, J., Qu, J., Liu, R., Qiang, Z., Liu, H., Zhao, X., 2009. Cu(II)-catalyzed THM formation

during water chlorination and monochloramination: a comparison study. J. Hazard Mater. 170 (1), 58–65.
Gallard, H., von Gunten, U., 2002. Chlorination of natural organic matter: kinetics of chlorination and of THM formation. Water Res. 36 (1), 65–74.
Ged, E.C., Chadik, P.A., Boyer, T.H., 2015. Predictive capability of chlorination disinfection byproducts models. J. Environ. Manag. 149, 253–262.
Gonce, N., Voudrias, E.A., 1994. Removal of chlorite and chlorate ions from water using granular activated carbon. Water Res. 28 (5), 1059–1069.
Gough, T.A., Webb, K.S., McPhail, M.F., 1977. Volatile nitrosamines from ion-exchange resins. Food Cosmet. Toxicol. 15 (5), 437–440.
Gui, L., Gillham, R.W., Odziemkowski, M.S., 2000. Reduction of N-nitrosodimethylamine with granular iron and nickel-enhanced iron. 1. Pathways and kinetics. Environ. Sci. Technol. 34 (16), 3489–3494.
Han, Y., Chen, Z.-l., Tong, L.-n., Yang, L., Shen, J.-m., Wang, B.-y., Liu, Y., Liu, Y., Chen, Q., 2013. Reduction of N-Nitrosodimethylamine with zero-valent zinc. Water Res. 47 (1), 216–224.
Han, Y., Chen, Z.-l., Shen, J.-m., Wang, J.-h., Li, W.-w., Li, J., Wang, B.-y., Tong, L.-n., 2017. The role of Cu(II) in the reduction of N-nitrosodimethylamine with iron and zinc. Chemosphere 167, 171–177.
Hanigan, D., Zhang, J., Herckes, P., Zhu, E., Krasner, S., Westerhoff, P., 2015. Contribution and removal of watershed and cationic polymer N-nitrosodimethylamine precursors. J. Am. Water Work. Assoc. 107 (3), 152–163.
Hozalski, R.M., Zhang, L., Arnold, W.A., 2001. Reduction of haloacetic acids by Fe0: implications for treatment and fate. Environ. Sci. Technol. 35 (11), 2258–2263.
Hu, J., Qiang, Z., Dong, H., Qu, J., 2016. Enhanced formation of bromate and brominated disinfection byproducts during chlorination of bromide-containing waters under catalysis of copper corrosion products. Water Res. 98, 302–308.
Hu, J.L., Chu, W.H., Sui, M.H., Xu, B., Gao, N.Y., Ding, S.k., 2018. Comparison of drinking water treatment processes combinations for the minimization of subsequent disinfection by-products formation during chlorination and chloramination. Chem. Eng. J. 335, 352–361.
Hua, G., Reckhow, D.A., 2007. Comparison of disinfection byproduct formation from chlorine and alternative disinfectants. Water Res. 41 (8), 1667–1678.
Hwang, S.C., Larson, R.A., Snoeyink, V.L., 1990. Reactions of free chlorine with substituted anilines in aqueous solution and on granular activated carbon. Water Res. 24 (4), 427–432.
Jackson, D.E., Larson, R.A., Snoeyink, V.L., 1987. Reactions of chlorine and chlorine dioxide with resorcinol in aqueous solution and adsorbed on granular activated carbon. Water Res. 21 (7), 849–857.
Jeong, C.H., Postigo, C., Richardson, S.D., Simmons, J.E., Kimura, S.Y., Mariñas, B.J., Barcelo, D., Liang, P., Wagner, E.D., Plewa, M.J., 2015. Occurrence and comparative toxicity of haloacetaldehyde disinfection byproducts in drinking water. Environ. Sci. Technol. 49 (23), 13749–13759.
Jiang, J., Zhang, X., Zhu, X., Li, Y., 2017. Removal of intermediate aromatic halogenated DBPs by activated carbon adsorption: a new approach to controlling halogenated DBPs in chlorinated drinking water. Environ. Sci. Technol. 51 (6), 3435–3444.
Jiang, J., Li, W., Zhang, X., Liu, J., Zhu, X., 2018. A new approach to controlling halogenated DBPs by GAC adsorption of aromatic intermediates from chlorine disinfection: effects of bromide and contact time. Separ. Purif. Technol. 203, 260–267.
Joo, S.H., Mitch, W.A., 2007. Nitrile, aldehyde, and halonitroalkane formation during chlorination/chloramination of primary amines. Environ. Sci. Technol. 41 (4), 1288–1296.
Kemper, J.M., Westerhoff, P., Dotson, A., Mitch, W.A., 2009. Nitrosamine, dimethylnitramine, and chloropicrin formation during strong base anion-exchange treatment. Environ. Sci. Technol. 43 (2), 466–472.
Kimoto, W.I., Dooley, C.J., Carré, J., Fiddler, W., 1980. Role of strong ion exchange resins in nitrosamine formation in water. Water Res. 14 (7), 869–876.
Klaus, L.E.K., Lawrence, J., 1977. Polyelectrolytes: potential chloroform precursors. Science 196 (4295), 1205–1206.
Kohut, K.D., Andrews, S.A., 2003. Polyelectrolyte age and N-nitrosodimethylamine formation in drinking water treatment. Water Qual. Res. J. Can. 38 (4), 719–735.
Korshin, G.V., Benjamin, M.M., Chang, H.-S., Gallard, H., 2007. Examination of NOM chlorination reactions by conventional and stop-flow differential absorbance spectroscopy. Environ. Sci. Technol. 41 (8), 2776–2781.
Krasner, S.W., Weinberg, H.S., Richardson, S.D., Pastor, S.J., Chinn, R., Sclimenti, M.J., Onstad, G.D., Thruston, A.D., 2006. Occurrence of a new generation of disinfection byproducts. Environ. Sci. Technol. 40 (23), 7175–7185.
Krasner, S.W., Mitch, W.A., McCurry, D.L., Hanigan, D., Westerhoff, P., 2013. Formation, precursors, control, and occurrence of nitrosamines in drinking water: a review. Water Res. 47 (13), 4433–4450.
Krasner, S.W., Shirkhani, R., Westerhoff, P., Hanigan, D., Mitch, W.A., McCurry, D.L., Chen, C., Skadsen, J., Gunten, U.V., 2015. Controlling the Formation of Nitrosamines during Water Treatment (Denver, Colorado).
Krasner, S.W., Leavey, S., Qian, Y., Li, X.F., Marfil-Vega, R., Bukhari, Z. (2016a) Nitrosamine Occurrence Survey, Denver, Colorado.
Krasner, S.W., Lee, T.C.F., Westerhoff, P., Fischer, N., Hanigan, D., Karanfil, T., Beitasandí, W., Tayloredmonds, L., Andrews, R.C., 2016b. Granular activated carbon treatment may result in higher predicted genotoxicity in the presence of bromide. Environ. Sci. Technol. 50 (17), 9583–9591.
Le Roux, J., Gallard, H., Croué, J.-P., 2011. Chloramination of nitrogenous contaminants (pharmaceuticals and pesticides): NDMA and halogenated DBPs formation. Water Res. 45 (10), 3164–3174.
Lee, J.-Y., Hozalski, R.M., Arnold, W.A., 2007. Effects of dissolved oxygen and iron aging on the reduction of trichloronitromethane, trichloracetonitrile, and trichloropropanone. Chemosphere 66 (11), 2127–2135.
Lee, J.-Y., Pearson, C.R., Hozalski, R.M., Arnold, W.A., 2008. Degradation of trichloronitromethane by iron water main corrosion products. Water Res. 42 (8), 2043–2050.
Lee, W., Westerhoff, P., 2006. Dissolved organic nitrogen removal during water treatment by aluminum sulfate and cationic polymer coagulation. Water Res. 40 (20), 3767–3774.
Lehtola, M.J., Nissinen, T.K., Miettinen, I.T., Martikainen, P.J., Vartiainen, T., 2004. Removal of soft deposits from the distribution system improves the drinking water quality. Water Res. 38 (3), 601–610.
Lemus Pérez, M.F., Rodríguez Susa, M., 2017. Exopolymeric substances from drinking water biofilms: dynamics of production and relation with disinfection by products. Water Res. 116, 304–315.
Li, B., Qu, J., Liu, H., Hu, C., 2007. Effects of copper(II) and copper oxides on THMs formation in copper pipe. Chemosphere 68 (11), 2153–2160.
Li, B., 2012. Charaterization of Pore Structure and Surface Chemistry of Activated Carbons - A Review.
Li, J.W., Yu, Z., Gao, M., Zhang, L., Cai, X., Chao, F., 1996. Effect of ultraviolet irradiation on the characteristics and trihalomethanes formation potential of humic acid. Water Res. 30 (2), 347–350.
Li, Q., Mahendra, S., Lyon, D.Y., Brunet, L., Liga, M.V., Li, D., Alvarez, P.J.J., 2008. Antimicrobial nanomaterials for water disinfection and microbial control: potential applications and implications. Water Res. 42 (18), 4591–4602.
Li, Z., Chen, T., Cui, F., Xie, Y., Xu, W., 2017. Impact of chitosan and polyacrylamide on formation of carbonaceous and nitrogenous disinfection by-products. Chemosphere 178, 26–33.
Liao, X., Chen, C., Xie, S., Hanigan, D., Wang, J., Zhang, X., Westerhoff, P., Krasner, S.W., 2015. Nitrosamine precursor removal by bac: a case study of adsorption versus biotreatment. J. Am. Water Work. Assoc. 107 (9), E454–E463.
Lin, J., Ellaway, M., Adrien, R., 2001. Study of corrosion material accumulated on the inner wall of steel water pipe. Corros. Sci. 43 (11), 2065–2081.
Lin, Y.-P., Washburn, M.P., Valentine, R.L., 2008. Reduction of lead oxide (PbO2) by iodide and formation of iodoform in the PbO2/I−/NOM system. Environ. Sci. Technol. 42 (8), 2919–2924.
Liu, C., von Gunten, U., Croué, J.-P., 2012. Enhanced bromate formation during chlorination of bromide-containing waters in the presence of CuO: catalytic disproportionation of hypobromous acid. Environ. Sci. Technol. 46 (20), 11054–11061.
Liu, C., von Gunten, U., Croué, J.-P., 2013a. Chlorination of bromide-containing waters: enhanced bromate formation in the presence of synthetic metal oxides and deposits formed in drinking water distribution systems. Water Res. 47 (14), 5307–5315.
Liu, C., von Gunten, U., Croué, J.-P., 2013b. Enhanced chlorine dioxide decay in the presence of metal oxides: relevance to drinking water distribution systems. Environ. Sci. Technol. 47 (15), 8365–8372.
Liu, C., Salhi, E., Croué, J.P., Von, G.U., 2014. Chlorination of iodide-containing waters in the presence of CuO: formation of periodate. Environ. Sci. Technol. 48 (22), 13173–13180.
Liu, C., Croué, J.-P., 2016. formation of bromate and halogenated disinfection byproducts during chlorination of bromide-containing waters in the presence of dissolved organic matter and CuO. Environ. Sci. Technol. 50 (1), 135–144.
Liu, C., Olivares, C.I., Pinto, A.J., Lauderdale, C.V., Brown, J., Selbes, M., Karanfil, T., 2017. The control of disinfection byproducts and their precursors in biologically active filtration processes. Water Res. 124, 630–653.
Liu, J., Zhang, X., 2014. Comparative toxicity of new halophenolic DBPs in chlorinated saline wastewater effluents against a marine alga: halophenolic DBPs are generally more toxic than haloaliphatic ones. Water Res. 65, 64–72.
Liu, S.-g., Zhu, Z.-l., Tan, X.-c., Feng, X.-h., Huang, Z.-y., Qiu, Y.-l., Zhao, J.-f., 2013c. The influence of Cu(II) on the formation and distribution of disinfection byproducts during the chlorination of drinking water. Water, Air, Soil Pollut. 224 (4), 1493.
Liu, S., Lim, M., Fabris, R., Chow, C., Drikas, M., Amal, R., 2008. TiO2 photocatalysis of natural organic matter in surface water: impact on trihalomethane and haloacetic acid formation potential. Environ. Sci. Technol. 42 (16), 6218–6223.
Liu, S., Gunawan, C., Barraud, N., Rice, S.A., Harry, E.J., Amal, R., 2016. Understanding, monitoring, and controlling biofilm growth in drinking water distribution systems. Environ. Sci. Technol. 50 (17), 8954–8976.
Ma, S., Guo, X., Chen, B., 2016. Toward better understanding of chloral hydrate stability in water: kinetics, pathways, and influencing factors. Chemosphere 157, 18–24.
Mallevialle, J., Bruchet, A., Fiessinger, F., xe, ois, 1984. How safe are organic polymers in water treatment? J. Am. Water Work. Assoc. 76 (6), 87–93.
Matheson, L.J., Tratnyek, P.G., 1994. Reductive dehalogenation of chlorinated methanes by iron metal. Environ. Sci. Technol. 28 (12), 2045–2053.
Matilainen, A., Vepsäläinen, M., Sillanpää, M., 2010. Natural organic matter removal by coagulation during drinking water treatment: a review. Adv. Colloid Interfac. 159 (2), 189–197.
McCreary, J.J., Snoeyink, V.L., 1981. Reaction of free chlorine with humic substances before and after adsorption on activated carbon. Environ. Sci. Technol. 15 (2), 193–197.
McCreary, J.J., Snoeyink, V.L., Larson, R.A., 1982. Comparison of the reaction of aqueous free chlorine with phenolic acids in solution and adsorbed on granular activated carbon. Environ. Sci. Technol. 16 (6), 339–344.
Metch, J.W., Ma, Y., Pruden, A., Vikesland, P.J., 2015. Enhanced disinfection by-

product formation due to nanoparticles in wastewater treatment plant effluents. Environ. Sci.: Water Res. Technol. 1 (6), 823–831.
Mitch, W.A., Sedlak, D.L., 2004. Characterization and fate of N-nitrosodimethylamine precursors in municipal wastewater treatment plants. Environ. Sci. Technol. 38 (5), 1445–1454.
Morran, J.I.M., Whittle, M., Fabris, R.B., Harris, M., Leach, J.S., Newcombe, G., Drikas, M., 2011. Nitrosamines from pipeline materials in drinking water distribution systems. J. Am. Water Work. Assoc. 103 (10), 76–83.
Muellner, M.G., Wagner, E.D., McCalla, K., Richardson, S.D., Woo, Y.T., Plewa, M.J., 2007. Haloacetonitriles vs. regulated haloacetic acids: are nitrogen-containing DBPs more toxic? Environ. Sci. Technol. 41 (2), 645–651.
Najm, I., Trussell, R.R., 2001. NDMA formation in water and wastewater. J. Am. Water Work. Assoc. 93 (2), 92–99.
Paciolla, M.D., Davies, G., Jansen, S.A., 1999. Generation of hydroxyl radicals from metal-loaded humic acids. Environ. Sci. Technol. 33 (11), 1814–1818.
Padhye, L., Wang, P., Karanfil, T., Huang, C.-H., 2010. Unexpected role of activated carbon in promoting transformation of secondary amines to N-nitrosamines. Environ. Sci. Technol. 44 (11), 4161–4168.
Padhye, L., Luzinova, Y., Cho, M., Mizaikoff, B., Kim, J.-H., Huang, C.-H., 2011. Poly-DADMAC and dimethylamine as precursors of N-nitrosodimethylamine during ozonation: reaction kinetics and mechanisms. Environ. Sci. Technol. 45 (10), 4353–4359.
Pan, B., Xing, B., 2008. Adsorption mechanisms of organic chemicals on carbon nanotubes. Environ. Sci. Technol. 42 (24), 9005–9013.
Pan, Y., Zhang, X., 2013. Four groups of new aromatic halogenated disinfection byproducts: effect of bromide concentration on their formation and speciation in chlorinated drinking water. Environ. Sci. Technol. 47 (3), 1265–1273.
Pan, Y., Zhang, X., Wagner, E.D., Osiol, J., Plewa, M.J., 2014. Boiling of simulated tap water: effect on polar brominated disinfection byproducts, halogen speciation, and cytotoxicity. Environ. Sci. Technol. 48 (1), 149–156.
Park, S.-H., Wei, S., Mizaikoff, B., Taylor, A.E., Favero, C., Huang, C.-H., 2009. Degradation of amine-based water treatment polymers during chloramination as N-nitrosodimethylamine (NDMA) precursors. Environ. Sci. Technol. 43 (5), 1360–1366.
Park, S.H., Padhye, L.P., Wang, P., Cho, M., Kim, J.-H., Huang, C.-H., 2015. N-nitrosodimethylamine (NDMA) formation potential of amine-based water treatment polymers: effects of in situ chloramination, breakpoint chlorination, and pre-oxidation. J. Hazard Mater. 282, 133–140.
Parker, K.M., Zeng, T., Harkness, J., Vengosh, A., Mitch, W.A., 2014. enhanced formation of disinfection byproducts in shale gas wastewater-impacted drinking water supplies. Environ. Sci. Technol. 48 (19), 11161–11169.
Pearson, C.R., Hozalski, R.M., Arnold, W.A., 2005. Degradation of chloropicrin in the presence of zero-valent iron. Environ. Toxicol. Chem. 24 (12), 3037–3042.
Pieri, P., Andra, S.S., Charisiadis, P., Demetriou, G., Zambakides, N., Makris, K.C., 2014. Variability of tap water residual chlorine and microbial counts at spatially resolved points of use. Environ. Eng. Sci. 31 (4), 193–201.
Plewa, M.J., Wagner, E.D., Muellner, M.G., Hsu, K.-M., Richardson, S.D., 2008. Disinfection By-Products in Drinking Water. American Chemical Society, pp. 36–50.
Plewa, M.J., Wagner, E.D., 2015. Recent Advances in Disinfection By-Products. American Chemical Society, pp. 3–23.
Qu, X., Alvarez, P.J.J., Li, Q., 2013. Applications of nanotechnology in water and wastewater treatment. Water Res. 47 (12), 3931–3946.
Richardson, S.D., Thruston, A.D., Collette, T.W., Patterson, K.S., Lykins, B.W., Ireland, J.C., 1996. Identification of TiO2/UV disinfection byproducts in drinking water. Environ. Sci. Technol. 30 (11), 3327–3334.
Richardson, S.D., Plewa, M.J., Wagner, E.D., Schoeny, R., DeMarini, D.M., 2007. Occurrence, genotoxicity, and carcinogenicity of regulated and emerging disinfection by-products in drinking water: a review and roadmap for research. Mutat. Res/Rev. Mutat. 636 (1–3), 178–242.
Richardson, S.D., Fasano, F., Ellington, J.J., Crumley, F.G., Buettner, K.M., Evans, J.J., Blount, B.C., Silva, L.K., Waite, T.J., Luther, G.W., McKague, A.B., Miltner, R.J., Wagner, E.D., Plewa, M.J., 2008. Occurrence and mammalian cell toxicity of iodinated disinfection byproducts in drinking water. Environ. Sci. Technol. 42 (22), 8330–8338.
Richardson, S.D., Postigo, C., 2012. In: Barceló, D. (Ed.), Emerging Organic Contaminants and Human Health. Springer Berlin Heidelberg, Berlin, Heidelberg, pp. 93–137.
Rook, J.J., 1974. Formation of haloforms during chlorination of natural water. Water Treat. Exam. 23, 234–243.
Rossman, L.A., Brown, R.A., Singer, P.C., Nuckols, J.R., 2001. DBP formation kinetics in a simulated distribution system. Water Res. 35 (14), 3483–3489.
Samatya, S., Kabay, N., Yüksel, Ü., Arda, M., Yüksel, M., 2006. Removal of nitrate from aqueous solution by nitrate selective ion exchange resins. React. Funct. Polym. 66 (11), 1206–1214.
Seidel, H.F., 1985. Water utility operating data: an analysis. J. Am. Water Work. Assoc. 77 (5), 34–41.
Selbes, M., Kim, D., Karanfil, T., 2014. The effect of pre-oxidation on NDMA formation and the influence of pH. Water Res. 66, 169–179.
Selcuk, H., Sarikaya, H.Z., Bekbolet, M., Anderson, M.A., 2006. Bromate formation on the non-porous TiO2 photoanode in the photoelectrocatalytic system. Chemosphere 62 (5), 715–721.
Selcuk, H., 2010. Disinfection and formation of disinfection by-products in a photoelectrocatalytic system. Water Res. 44 (13), 3966–3972.
Sgroi, M., Roccaro, P., Oelker, G.L., Snyder, S.A., 2015. N-nitrosodimethylamine (NDMA) formation at an indirect potable reuse facility. Water Res. 70, 174–183.
Shah, A.D., Mitch, W.A., 2012. Halonitroalkanes, halonitriles, haloamides, and N-nitrosamines: a critical review of nitrogenous disinfection byproduct formation pathways. Environ. Sci. Technol. 46 (1), 119–131.
Sharma, V.K., Yang, X., Cizmas, L., McDonald, T.J., Luque, R., Sayes, C.M., Yuan, B., Dionysiou, D.D., 2017. Impact of metal ions, metal oxides, and nanoparticles on the formation of disinfection byproducts during chlorination. Chem. Eng. J. 317, 777–792.
Snoeyink, V.L., Clark, R.R., McCreary, J.J., McHie, W.F., 1981. Organic compounds produced by the aqueous free-chlorine-activated carbon reaction. Environ. Sci. Technol. 15 (2), 188–192.
Sokolowski, A., Gora, S., Andrews, S., 2014. In: Hu, A., Apblett, A. (Eds.), Nanotechnology for Water Treatment and Purification. Springer International Publishing, Cham, pp. 275–306.
Soponkanaporn, T., Gehr, R., 1988. In: Lijklema, L., Imhoff, K.R., Ives, K.J., Jenkins, D., Ludwig, R.G., Suzuki, M., Toerien, D.F., Wheatland, A.B., Milburn, A., Izod, E.J. (Eds.), Water Pollution Research and Control Brighton. Pergamon, pp. 857–868.
Stüber, F., Font, J., Fortuny, A., Bengoa, C., Eftaxias, A., Fabregat, A., 2005. Carbon materials and catalytic wet air oxidation of organic pollutants in wastewater. Top. Catal. 33 (1), 3–50.
Summers, R.S., Benz, M.A., Shukairy, H.M., Cummings, L., 1993. Effect of separation processes on the formation of brominated THMs. J. Am. Water Work. Assoc. 85 (1), 88–95.
Sun, H., Liu, H., Han, J., Zhang, X., Cheng, F., Liu, Y., 2018. Chemical cleaning-associated generation of dissolved organic matter and halogenated byproducts in ceramic MBR: ozone versus hypochlorite. Water Res. 140, 243–250.
Symons, J.M., Krasner, S.W., Simms, L.A., Sclimenti, M., 1993. Measurement of THM and precursor concentrations revisited: the effect of bromide ion. J. Am. Water Work. Assoc. 85 (1), 51–62.
Takht Ravanchi, M., Kaghazchi, T., Kargari, A., 2009. Application of membrane separation processes in petrochemical industry: a review. Desalination 235 (1), 199–244.
Tang, S., Wang, X.-m., Mao, Y.-q., Zhao, Y., Yang, H.-w., Xie, Y.F., 2015. Effect of dissolved oxygen concentration on iron efficiency: removal of three chloroacetic acids. Water Res. 73, 342–352.
Tang, S., Wang, X.-m., Liu, S.-t., Yang, H.-w., Xie, Y.F., Yang, X.-y., 2017. Mechanism and kinetics of halogenated compound removal by metallic iron: Transport in solution, diffusion and reduction within corrosion films. Chemosphere 178, 119–128.
Teefy, S., Chan Clifford, C., Wong, W., Work, L., 2014. NDMA formation from gaskets used in water storage tanks. J. Am. Water Work. Assoc. 106 (9), 408–417.
Tofighy, M.A., Mohammadi, T., 2011. Adsorption of divalent heavy metal ions from water using carbon nanotube sheets. J. Hazard Mater. 185 (1), 140–147.
Toroz, I., Uyak, V., 2005. Seasonal variations of trihalomethanes (THMs) in water distribution networks of Istanbul City. Desalination 176 (1), 127–141.
Tugulea, A.M., Bérubé, D., Giddings, M., Lemieux, F., Hnatiw, J., Priem, J., Avramescu, M.L., 2014. Nano-silver in drinking water and drinking water sources: stability and influences on disinfection by-product formation. Environ. Sci. Pollut. Res. 21 (20), 11823–11831.
USEPA, 2006. Stage 2 disinfectants and disinfection byproducts rule: National primary and secondary drinking water regulations: final rule. Fed. Regist. 71 (2).
USEPA, 2007. Distribution System Inventory, Integrity and Water Quality. http://www.epa.gov/safewater/disinfection/lt2/compliance.html.
Vel Leitner, N.K., De Laat, J., Dore, M., Suty, H., Pouillot, M., 1994. Inorganic and organic byproducts of the reactions between chlorite, activated carbon, and phenolic compounds. Environ. Sci. Technol. 28 (2), 222–230.
Verdugo, E.M., Krause, C., Genskow, K., Han, Y., Baltrusaitis, J., Mattes, T.E., Valentine, R.L., Cwiertny, D.M., 2014. N-functionalized carbon nanotubes as a source and precursor of N-nitrosodimethylamine: implications for environmental fate, transport, and toxicity. Environ. Sci. Technol. 48 (16), 9279–9287.
Verdugo, E.M., Nelson, K.J., Bako, C.M., Valentine, R.L., Cwiertny, D.M., 2016. Formation of trihalomethanes and haloacetic acids during chlorination of functionalized carbon nanotubes. Environ. Sci.: Nano 3 (6), 1327–1339.
Voudrias, E.A., Larson, R.A., Snoeyink, V.L., 1985a. Effects of activated carbon on the reactions of free chlorine with phenols. Environ. Sci. Technol. 19 (5), 441–449.
Voudrias, E.A., Larson, R.A., Snoeyink, V.L., 1985b. Effects of activated carbon on the reactions of combined chlorine with phenols. Water Res. 19 (7), 909–915.
Wagner, E.D., Plewa, M.J., 2017. CHO cell cytotoxicity and genotoxicity analyses of disinfection by-products: an updated review. J. Environ. Sci. 58, 64–76.
Walter, R.K., Lin, P.-H., Edwards, M., Richardson, R.E., 2011. Investigation of factors affecting the accumulation of vinyl chloride in polyvinyl chloride piping used in drinking water distribution systems. Water Res. 45 (8), 2607–2615.
Wang, C., Shang, C., Ni, M., Dai, J., Jiang, F., 2012. (Photo)chlorination-Induced physicochemical transformation of aqueous fullerene nC60. Environ. Sci. Technol. 46 (17), 9398–9405.
Wang, C., Yang, X., Zheng, Q., Moe, B., Li, X.-F., 2018. Halobenzoquinone-induced developmental toxicity, oxidative stress, and apoptosis in zebrafish embryos. Environ. Sci. Technol. 52 (18), 10590–10598.
Wang, J.-J., Liu, X., Ng, T.W., Xiao, J.-W., Chow, A.T., Wong, P.K., 2013. Disinfection byproduct formation from chlorination of pure bacterial cells and pipeline biofilms. Water Res. 47 (8), 2701–2709.
Wang, W., Zhu, L., 2010. Effect of zinc on the transformation of haloacetic acids (HAAs) in drinking water. J. Hazard Mater. 174 (1), 40–46.
Wang, X., Mao, Y., Tang, S., Yang, H., Xie, Y.F., 2015. Disinfection byproducts in drinking water and regulatory compliance: a critical review. Front. Environ. Sci.

Eng. 9 (1), 3–15.
WHO, 2004. Water, Sanitation and hygiene links to health : facts and figures. http://www.who.int/water_sanitation_health/factsfigures2005.pdf.
Wilczak, A., Assadi-Rad, A., Lai, H.H., Hoover, L.L., Smith, J.F., Berger, R., Rodigari, F., Beland, J.W., Lazzelle, L.J., Kincannon, E.G., Baker, H., Heaney, C.T., 2003. formation of NDMA in chloraminated water coagulated with DADMAC cationic polymer. J. Am. Water Work. Assoc. 95 (9), 94–106.
Xia, Y., Lin, Y.-L., Xu, B., Hu, C.-Y., Gao, Z.-C., Chu, W.-H., Gao, N.-Y., 2017. Iodinated trihalomethane formation during chloramination of iodate-containing waters in the presence of zero valent iron. Water Res. 124, 219–226.
Xie, P., de Lannoy, C.-F., Ma, J., Wiesner, M.R., 2015. Chlorination of polyvinyl pyrrolidone–polysulfone membranes: organic compound release, byproduct formation, and changes in membrane properties. J. Membr. Sci. 489, 28–35.
Yang, M.T., Zhang, X.R., 2013. Comparative developmental toxicity of new aromatic halogenated DBPs in a chlorinated saline sewage effluent to the marine polychaete platynereis dumerilii. Environ. Sci. Technol. 47 (19), 10868–10876.
Yang, M.T., Zhang, X.R., 2014. Halopyrroles: a new group of highly toxic disinfection byproducts formed in chlorinated saline wastewater. Environ. Sci. Technol. 48 (20), 11846–11852.
Yang, X., Fan, C., Shang, C., Zhao, Q., 2010. Nitrogenous disinfection byproducts formation and nitrogen origin exploration during chloramination of nitrogenous organic compounds. Water Res. 44 (9), 2691–2702.
Yu, Y., Reckhow, D.A., 2015. Kinetic analysis of haloacetonitrile stability in drinking waters. Environ. Sci. Technol. 49 (18), 11028–11036.
Zeng, T., Pignatello, J.J., Li, R.J., Mitch, W.A., 2014. Synthesis and application of a quaternary phosphonium polymer coagulant to avoid N-nitrosamine formation. Environ. Sci. Technol. 48 (22), 13392–13401.
Zeng, T., Li, R.J., Mitch, W.A., 2016. Structural modifications to quaternary ammonium polymer coagulants to inhibit N-nitrosamine formation. Environ. Sci. Technol. 50 (9), 4778–4787.
Zeng, T., Mitch, W.A., 2016. Impact of nitrification on the formation of N-nitrosamines and halogenated disinfection byproducts within distribution system storage facilities. Environ. Sci. Technol. 50 (6), 2964–2973.
Zhang, H., Andrews, S.A., 2012. Catalysis of copper corrosion products on chlorine decay and HAA formation in simulated distribution systems. Water Res. 46 (8), 2665–2673.
Zhang, H., Andrews, S.A., 2013. Factors affecting catalysis of copper corrosion products in NDMA formation from DMA in simulated premise plumbing. Chemosphere 93 (11), 2683–2689.
Zhang, L., Arnold, W.A., Hozalski, R.M., 2004. Kinetics of haloacetic acid reactions with Fe(0). Environ. Sci. Technol. 38 (24), 6881–6889.
Zhang, Y.M., Chu, W.H., Yao, D.C., Yin, D.Q., 2017. Control of aliphatic halogenated DBP precursors with multiple drinking water treatment processes: formation potential and integrated toxicity. J. Environ. Sci. 58, 322–330.
Zhao, Y., Yang, H.-w., Liu, S.-t., Tang, S., Wang, X.-m., Xie, Y.F., 2016. Effects of metal ions on disinfection byproduct formation during chlorination of natural organic matter and surrogates. Chemosphere 144, 1074–1082.